UNIVERSITY OF LISBON
FACULTY OF SCIENCES

BIOMEDICAL ENGINEERING AND BIOPHYSICS

INTERNSHIP REPORT

MULTISCALE ANALYSIS OF HEART RATE DYNAMICS

Filipa da Conceição dos Santos Rodrigues

September 2012

UNIVERSITY OF LISBON
FACULTY OF SCIENCES
BIOMEDICAL ENGINEERING AND BIOPHYSICS

INTERNSHIP REPORT

MULTISCALE ANALYSIS OF HEART RATE DYNAMICS

Filipa da Conceição dos Santos Rodrigues

September 2012

Supervisors: Dr. Madalena Costa[1] and Dr. Ary Goldberger[1]
InternshipProgramCoordinator: Professor Eduardo Ducla-Soares[2]

[1]Beth Israel Deaconess Medical Center, Harvard Medical School, Boston, USA
[2]Institute of Biophysics and Biomedical Engineering, Faculty of Sciences of the University of Lisbon, Lisbon, Portugal

Contents

Abstract

The extraction of accurate information concerning the health status of a patient from a set of heart rate signals is an important challenge in cardiology. Due to the nonlinearity, nonstationarity and multiscale characteristics of the physiological signals, it also becomes a challenge to analyze this type of data. In this report, a multiscale approach is suggested to study the fetal heart rate (FHR) and the heart rate variability (HRV) in order to distinguish healthy and unhealthy subjects.

It is known that healthy systems are more complex than unhealthy ones. Based on this assumption, for the FHR analysis a compression-based algorithm and the Multiscale entropy (MSE) method were applied in order to quantify the complexity of healthy and acidemic fetuses. Contrary to the compression-based algorithm, the MSE analysis along with a moving window procedure was able to distinguish healthy from acidemic cases, confirming the hypothesis that healthy systems are more complex than unhealthy systems.

For the HRV analysis, Poincaré Plot (PP) technique was used. The PP is one of the most important techniques used for visually representing the heart rate variability. Inspired in the MSE method, a multiscale PP was used, i.e., the PP technique was applied to the coarse-grained time series of the cardiac interbeat intervals of different groups of subjects, in order to study the evolution of the geometry of these PPs over the scales. Healthy subjects showed an invariable geometry for the different scales, which reflects the fractal nature of the healthy systems. In the other hand, subjects with atrial fibrillation, exhibit a PP that decreases its area across the scales, reflecting the loss of complexity. The fitting ellipse technique was used to quantify the geometry of these PPs, but it proved to be a very limited method. The Empirical Mode Decomposition (EMD) was also used to quantify the variability of the several frequencies components of the heart rate, during the day and night periods. This method confirmed that the HRV of healthy systems is higher that healthy elderly and subjects with heart diseases.

List of Abbreviations

ApEN – Approximate Entropy

CI – Complexity Index

CTG – Cardiotocograph

EMD – Empirical Mode Decomposition

FHR – Fetal Heart Rate

HRV – Heart Rate Variability

IMF –Independent Mode Function

MSE – Multiscale Entropy

PP – Poincaré Plot

SampEn – Sample Entropy

SD – Standard Deviation

List of Figures

Acknowledgements

I am deeply grateful to Dr. Madalena Costa and Dr. Ary Goldberger for letting me work with them at the Wyss Institute for Biologically Inspired Engineering at Harvard University, and also for their teaching, enthusiasm and welcoming. I would also like to thank Anton Burykin for all support and inspiring conversations and Maria Inês Meyer for her friendship.

I am also very grateful to Professor Eduardo Ducla-Soares for this unique opportunity, for his encouragement and support.

I would like to thank the Rectorate of the University of Lisbon, Calouste Gulbenkian Foundation and the Wyss Institute for the financial support.

Finally, I would like to express my deepest gratitude to all my closest friends and family for their love and unconditional support.

1. Introduction

1.1 Work Context

This report is the result of the summer internship required for the Bachelor's Degree in Biomedical Engineering and Biophysics at the Faculty of Sciences of the University of Lisbon. Professor Eduardo Ducla-Soares was the internship program coordinator.

The internship took place from 31th June to September 9th, at the Wyss Institute for Biologically Inspired Engineering at Harvard University, in Boston, Massachusetts, United States of America. The institution's mission is to develop biologically inspired materials and devices that will solve critical medical and environmental problems and to translate these transformative technologies into products that have an impact on society and the world[1].

The internship was supervised by Dr. Madalena Costa and Dr. Ary Goldberger. Dr. Madalena Costa is an Assistant Professor of Medicine at Harvard Medical School, Division of Interdisciplinary Medicine and Biotechnology, Beth Israel Deaconess Medical Center. She is also Associate Director of the Margret and H. A. Rey Institute for Nonlinear Dynamics in Medicine. Dr. Ary Goldberger is the Director of the Rey Laboratory and Professor of Medicine at the Harvard Medical School. He is the Program Director of the Research Resource for Complex Physiologic Signals[1] funded by the National Institute of Biomedical Imaging and Bioengineering and National Institute of General Medical Sciences of the National Institutes of Health. He is also a core faculty member of the Wyss Institute for Biologically Inspired Engineering at Harvard University.

The multiscale analysis of the heart rate dynamics was the aim of the project developed in the internship. This analysis was accomplished in two different parts that involved a practical and a theoretical approach.

The practical part lied on developing more accurate ways to distinguish between healthy and unhealthy fetuses by analyzing the fetal heart rate tracings. This project is inserted in the HMS-Portugal[2] program. This program is a wide-ranging initiative that involves professors, researchers and students from the 7 schools of medicine in Portugal, as well as the country's main biomedical research laboratories [2].

[1] http://www.physionet.org

[2] Harvard Medical School Portugal

At Harvard University, the program involves researchers from Harvard Medical School and affiliated institutions together with faculty and students from the Faculty of Arts and sciences, the Harvard School of Public Health, and the Kennedy School of Government [2].The final goal of this project inserted in the HMS Portugal program, is to improve perinatal decision-making by developing complexity-based dynamical measures and novel acquisition systems. The hypothesis was that heart rate dynamics of healthy fetuses are more complex than the unhealthy ones. In order to test this hypothesis, compression algorithms and multiscale entropy method (MSE) were applied to the FHR tracings.

The theoretical part consisted in plotting Poincaré Maps of the cardiac interbeat (RR) intervals of healthy and unhealthy subjects and attempt to quantify the geometry of these plots. The hypothesis was that the healthy systems contain information in multiscale, and the unhealthy systems contain information only in the shortest scale. To test this hypothesis, multiscale Poincaré Maps were plotted.

1.2 Motivation

The analysis of physiological signals is very changeling due to their nonlinearity, nonstationarity and multiscale characteristics. In this report, the fetal heart rate (FHR) and the heart rate variability (HRV) are study with a multiscale approach.

The FHR monitoring is of great clinical importance, since a correct diagnosis can prevent complications during labor. Labor is a time of risk for asphyxia and asphyxia-related morbidity and mortality due to the uterine contractions. The risk of complications such as neurological injuries increases when gas exchange during labor is impaired enough to cause metabolic acidosis (indicating asphyxia)[3].The dying fetus does not always have a specific FHR pattern, so it is not possible to use FHR tracing alone to be certain that prompt intervention will result in a normal neonatal outcome. For this reason the most frequent problems are related to FHR interpretations because oftentimes there is no consensus between doctors over FHR tracing analysis [4]. This may result in a late intervention which can deal with severe consequences to the fetus, or, in the other hand, in unnecessary surgical interventions such as cesarean sections.

The HRV is an important variable in diagnosis. For example, it is accepted that HRV is reduced in patients with diabetes and autonomic dysfunction and the higher the HRV, the better prognosis in survivors of myocardial infarction or patients with heart failure [5]. The Poincaré plot (PP) is a technique widely used in the context of medical sciences to quantify the HRV. The PP is a visual technique that summarizes the entire recording and make possible to extract the information on short and long time behavior of the heart action [5]. This technique is applied to the whole RR intervals time series.However, it is known that the physiological systems contain information over

multiple scales. Although the PP is a valuable HRV analysis technique due to its ability to display nonlinear aspects of the interval sequence, it's very difficult to quantitatively characterize the plot to capture those nonlinearities.

1.3 Aim of the Project

The first part of the project was mainly related with the FHR tracing and interpretation. The aim was to developed an algorithm which distinguishes between healthy and unhealthy fetuses earlier as possible in order to increase the predictive capacity of the physicians to a successful intervention.

The second part of the project was inspired on the multiscale entropy analysis. The aim was to apply the PP technique of the RR intervals in multiple scales. PP geometry quantifying is also proposed in this project.

1.4 Approach

The purpose of this project was to apply the multiscale analysis to study the heart rate dynamics. On the first part of the project, the multiscale analysis was used to distinguish between healthy and unhealthy fetuses. On the second part of the project, the multiscale analysis was used to distinguish between healthy subjects and subjectswith heart diseases, and between healthy young and healthy old subjects.In order to analyze physiologic time series, C.-K.Peng, Madalena Costa and Ary L. Goldberger hypothesized the following [6]:

1. The complexity of a biological system reflects its ability to adapt and function in an ever-changing environment;
2. Biological systems need to operate across multiple scales of space and time, and hence their complexity is also multiscale and hierarchical;
3. A wide class of disease states, as well as aging, appear to degrade this biological complexity and reduce the adaptive capacity of the system. Thus, *loss of complexity* may be a generic, defining feature of pathologic dynamics, and the basis of new diagnostic, prognostic, and therapeutic approaches.

Based on the previous assumptions, the hypotheses established in this project were:

1. The FHR of healthy fetuses are more complex than the FHR of the acidemic fetuses;
2. The dynamics of healthy young subjects is more complex than healthy elder and patients with heart diseases such as CHF and AF. It is also expected the dynamics of healthy young subjects to be closer to 1/f (fractal) noise.

To verify these hypotheses, multiscale analysis was performed in both parts of the project. On the first part, the complexity of the FHR was measured using a compression algorithm and the MSE analysis. It is expected the healthy fetuses to have a higher complexity index value than the unhealthy ones. On the second part, Poincaré Plot of the RR intervals over multiple scales was performed. Graphically is expected that the geometry of the PP of healthy cases not to change across the scales, since the healthy cases are more complex and exhibit information in multiple scales. On the other hand, it is expected that the geometry of the PP of unhealthy cases to change, decreasing the area over the scales, since this cases only exhibit correlation in short term, i.e., they only have information on the first scales. It is also expected the geometry of the healthy group to be different from the unhealthy group due to the heart rate patterns.

2. Background

2.1 Physiological Concepts

The heart rate monitoring is extremely important in medical sciences' area. In order to improve the intervention of physicians, it is important to create automate and accurate methods to distinguish between healthy and unhealthy subjects. To achieve this, first of all is necessary to study the underling physiological concepts of the heart rate.

In this chapter, basic physiological concepts, such as heart rate variability, complexity of physiologic signals and some heart diseases will be discussed.

2.1.1 Heart Rate Variability

Heart beats are caused by electrical depolarization of the heart muscle, and the depolarization of the different parts of the heart can be observed in an electrocardiogram (ECG)(Fig.1)[5].

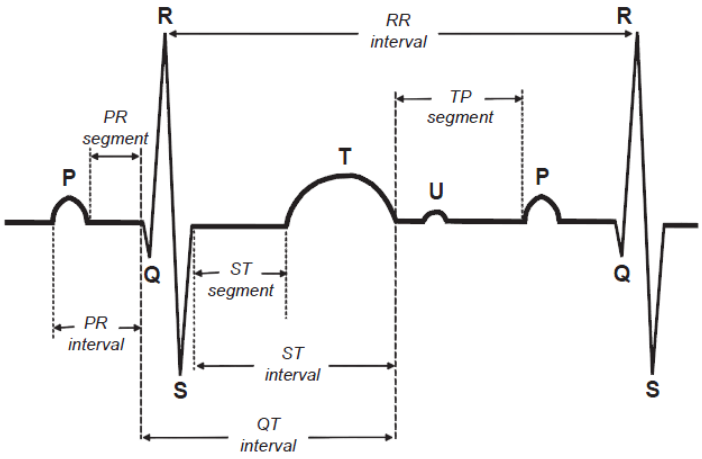

Fig.1.A schematic representation of a normal ECG. The P wave represents the depolarization of cardiac atria. The QRS complex characterizes depolarization of cardiac ventricles. T wave shows the ventricles' repolarization and U wave represents the late activation of the ventricles. [7]

The depolarization of atria is visualized by the P-wave. The Q, R and S waves create the QRS complex, which represents the depolarization of the ventricles. The interval between successive heart beats, i.e., the distance between consecutive QRS complexes is called RR interval [5]. The sinus node is the main rhythm generator, also called primary pacemaker, in healthy people. Although the primary pacemaker in a

physiological point of view is the fastest, there are other pacemakers with their own depolarizing activity [5]. This is very important, since if for any reason the sinus node fails to generate the excitatory signal, then secondary or tertiary centers with lower pacemaker's frequency initiate the main depolarization wave of the heart [5]. In a healthy person, the main excitatory wave depolarizes all potential pacemakers reducing theirs spontaneous depolarizing activity to 0, preventing the generation of non-sinus beat [5].

The heart rate and the duration of the RR interval depends on the interaction between the activity of the sinus node and the autonomic nervous system, substances circulating in the blood and present in the heart tissue. Breathing is the most important factor modulating heart rate. During the inspiration it causes heart rate acceleration and during the expiration it causes heart rate deceleration. The control of heart rate is also modulated by sympathetic and parasympathetic branches of autonomic system as well as many other reflexes [5]. All these systems and reflexes are the HRV, which refers to the fluctuations in the duration of RR interval from one beat to another [7]. Hence, HRV analysis enables clinicians to examine the influences of autonomic activity in heart rate [8].

2.1.2 Congestive Heart Failure

Congestive heart failure (CHF) is associated with an inability of the heart to empty itself adequately, resulting in the decrease of the effective work done by the heart muscle [9].Neurohormonal systems are activated to maintain cardiac output and tissue perfusion. However, chronic neurohormonal activation contributes to progressively deteriorating CHF. High sympathetic activity, neuroendocrine dysfunction, elevated cytokine levels and reduced vagal-cardiac activity contribute to decrease the HRV of patients with CHF [8].

2.1.3 Atrial Fibrillation

Atrial fibrillation (AF) is the most common cardiac arrhythmia [10].Arrhythmia is any heart rhythm that is not the sinus rhythm. AF is a type of atrial arrhythmia that is a fast, chaotic and disorganized atrial rhythm, without the capacity to generate effective atrial contractions [10].

2.1.4 Fetal Acidemia

An umbilical artery pH value less than 7.05 identifies a situation of fetal acidemia which indicates an impairment of placental gas exchange. Neonatal morbidity and risk of complications such as neurological injuries increases with occurrence of fetal acidemia. The risk increases during labor due to the uterine

contractions [3]. For this reason, FHR monitoring is essential during labor as well as an accurate interpretation of the FHR tracing.

2.2 Complexity Measurements

Two physiological time series could have identical variances and mean values and still have completely different patterns. In these cases, statistical analysis is not enough to characterize the time series. In Fig.2, the heart rate of two different subjects during sleep are represented. One is healthy and the other has a medical condition called obstructive sleep apnea in which intermittent collapse of the upper airway leads to cessation of effective breathing[12].

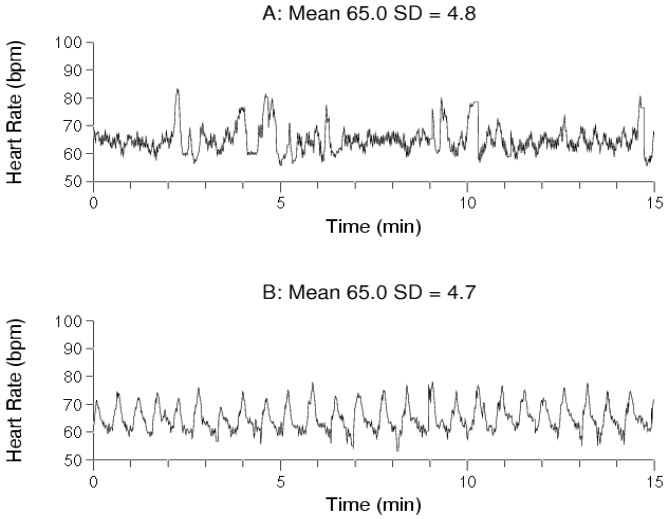

Fig.2. Two heart rate time series with identical means and variances. The upper is from a healthy subject; the bottom is from a subject with sleep apnea. [12]

The two heart rate sequences have nearly identical mean values and variances for the given observation but they look different to visual inspection. One way to capture the time series patterns, which is related to the dynamics of a system, is to quantify its complexity. In the context of physiological time series analysis, complexity is associated with meaningful structural richness incorporating correlations over multiple spatio-temporal scales, although there is no formal definition of the term complexity [11]. This biological complexity reflects the ability to adapt and function in an ever-changing environment [6].

Physiological information contained by the signal can be evaluated measuring its complexity. Compression-based and entropy-based measures are a powerful tool to evaluate the dynamics of both healthy and diseased biological systems. This analysis

can also provide a diagnostic, since healthy and unhealthy physiological signals have very different patterns, hence different complexity levels.

In this chapter, two different types of signal complexity measurements will be discussed: compression-based (Paq8l algorithm) and entropy-based measures (multiscale entropy).

2.2.1 Compression-based measures

One way of measuring the complexity is to quantify the degree of compressibility of the signal. This approach is based on the information theory which states that simple sequences can be described concisely and complex sequences cannot [12], i.e., a simple time series (not particularly complex) can be described concisely, since it contains no "surprises" and its information content is low. On the other hand, a complex time series requires lengthy descriptions, it is full of "surprises" and its information content is high. The process of removing a sample from the time series estimating its value using the information contained in the rest of the series is easier for a simple time series than for a complex one [12].

There are several types of compression algorithm. The one used in this report is the Paq8l algorithm[13]. The Paq8l is a type of a lossless compression algorithm, which means that there is no loss of information and the exact original data can be reconstructed from the compressed data. The Paq8l algorithm involves a lot of non-trivial mathematical operations , but its essence is based on statistical models to predict the next value in a time series[32]. The Compression Ratio can be used to quantify the degree of complexity and it's defined as

$$Compression\ Ratio = \frac{Compressed\ size}{Uncompressed\ size}$$

where Compressed Size is the size of the signal after the compression algorithm is applied and the Uncompressed Size is the original size of the signal. A simple signal is easier to compress since the information content is low. Consequently, the simpler the signal the lower is the compression ratio. Accordingly with this theory, the most compressible signals, such as constant or periodic signals, are the least complex. However, random uncorrelated signals, such as white noise, contain no information but are totally incompressible. This happens because it's not possible to estimate what value comes next in the series once it is completely random. Thus, white noise is considered an extremely complex signal, but it's known that this type of signal doesn't contain information, therefore it's not exhibit complexity. This is the major setback of using compression ration as a measure of complexity of a signal [12].

2.2.2 Entropy-based measures

Traditional entropy-based measurements, such as Approximate Entropy (ApEn) and Sample Entropy (SampEn), quantify the regularity of a time series. Entropy increases with the degree of disorder of a time series. For a random system the entropy has its maximum value and for a constant signal the entropy has its minimum value. However, an increase in the entropy may not always be associated with an increase in dynamical complexity [14]. For instance, white noise, which is a random and uncorrelated time series, has high entropy even though it doesn't exhibit any complexity.

Diseased systems often show a more regular behavior(Fig.3 (b)), thus they have lower entropy than healthy systems.However, some pathologies such as atrial fibrillation (Fig.3 (c)), shows an irregular behavior, thus its entropy value is higher than healthy systems (Fig.3 (a)), although the latter is more physiologically complex once it represents adaptive states.

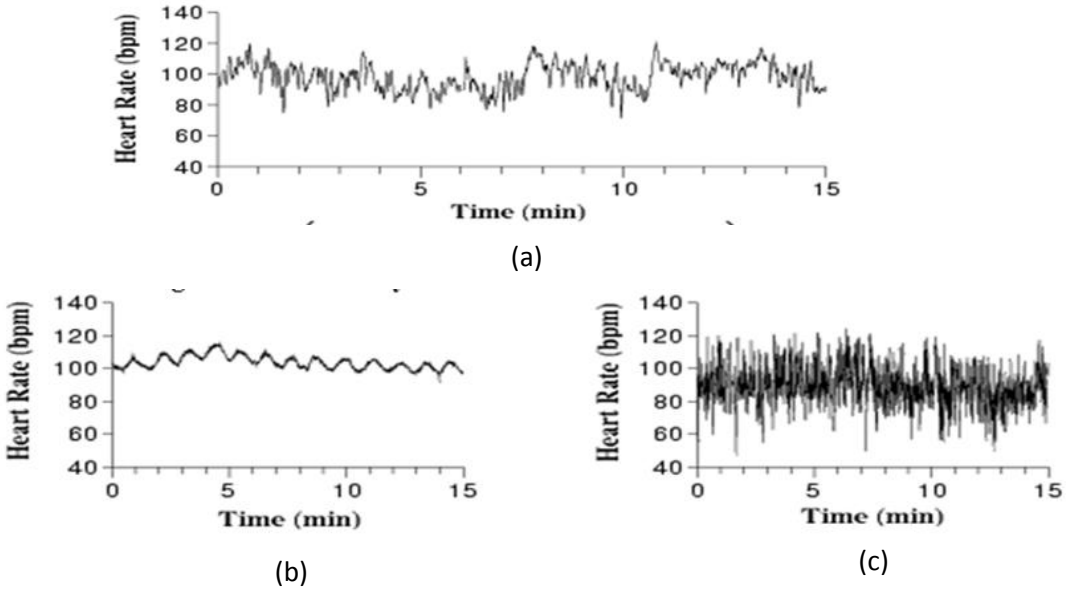

Fig.3. Heart rate interval from a (a) healthy subject; (b) subject with congestive heart failure; (c) subject with atrial fibrillation. The pattern of the heart rate from a healthy subject is not completely periodic neither completely random. Adapted from [12].

This inconsistency is due to the fact that traditional entropy measurements are based on single-scale analysis and do not take into account the complex temporal fluctuations inherent in healthy physiologic control systems [14]. Consequently, traditional entropy-based methods fail to evaluate the complexity of physiologic signals.

2.2.2.1 Multiscale Entropy

Multiscale entropy (MSE), different from traditional entropy-based measures, is based on multiple scale analysis that reveals the dependence of entropy on scale, which is crucial to correctly quantify the complexity of the signals [14].

The MSE method includes two procedures [15]:

1. A "coarse-graining" process is applied to the time series (Fig.4). This method involves constructing coarse-grained time series by averaging a successively increasing number of data points in non-overlapping windows, according to the equation:

$$y_j^{(\tau)} = \frac{1}{\tau} \sum_{i=(j-1)\tau+1}^{j\tau} x_i \ , \qquad 1 \le j \le \frac{N}{\tau}$$

The length of each coarse-grained time series $y_j^{(\tau)}$ is equal to the original time series x_i divided by a scale factor τ. For $\tau = 1$, the coarse-grained times series is simple the original time series.

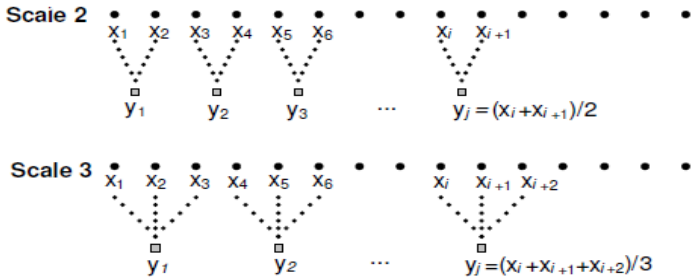

Fig.4. Schematic representation of the coarse-grained procedure for scale 2 and scale 3. [15]

2. Then multiscale entropy analysis is applied. This method involves the calculation of the entropy value, for each coarse-grained time series and plots it as a function of scale factor. To calculate the entropy valueSampEn is used. It looks for patterns in each coarse-grained series and quantifies their degree of regularity [16].SampEn for each scale is defined by the equation [17]:

$$SampEn\ (m, r, N) = -ln\left[\frac{A^m(r)}{B^m(r)}\right]$$

Where m is the length of each vector, N is the original length of the time series,$B^m(r)$is the total number of template matches of length m and $A^m(r)$ is total number of forward matches of length m+1. Thus, the quantity $\frac{A^m(r)}{B^m(r)}$is the conditional probability that two sequences within a tolerance r for m points remain within r of each other at next point m+1[17].Because it's a probability, the value of the fraction $\frac{A^m(r)}{B^m(r)}$ is between 0 and 1. Therefore, the quantity $-ln\left[\frac{A^m(r)}{B^m(r)}\right]$ will vary between 0 and$+\infty$.

Fig.5 illustrates the procedure for calculating sample entropy. In this example, the length, m, is 2 and the similarity criterion, r, is 20. The value of r is typically chosen to be between 10% and 20% of the standard deviation [16]. Dotted horizontal lines around data points u[1], u[2] and u[3] represent u[1]$\pm$r, u[2]$\pm$r and u[3]$\pm$r respectively. Two data points match each other, i.e., are indistinguishable, if the absolute difference between them is r. In green are represented all the points that match with the data point u[1], in red are represented all the data points that match with u[2] and in blue are represented all the data points that match with u[3]. As is shown in the figure, there are two green-red sequences, (u[13], u[14]) and (u[43], u[44]), that match the template sequence (u[1], u[2]) but only one green-red-blue sequence (u[43], u[44], u[45]) that matches the template sequence (u[1], u[2], u[3]). Thus, the number of sequences matching the 2-component template sequences is 2 and the number of sequences matching the 3-compontent template is 1. Then, these calculations are repeated for the next 2-component and 3-component template sequence, which are, (u[2],u[3]) and (u[2], u[3], u[4]), respectively. The numbers of sequences that match each 2 and 3-component, are counted and added to the previous values. This procedure is repeated for all the other possible template sequences, to determine the ratio between the total number of 2-component template matches and the total number of 3-componente template matches. The SampEn value is the natural logarithm of this ratio [16].

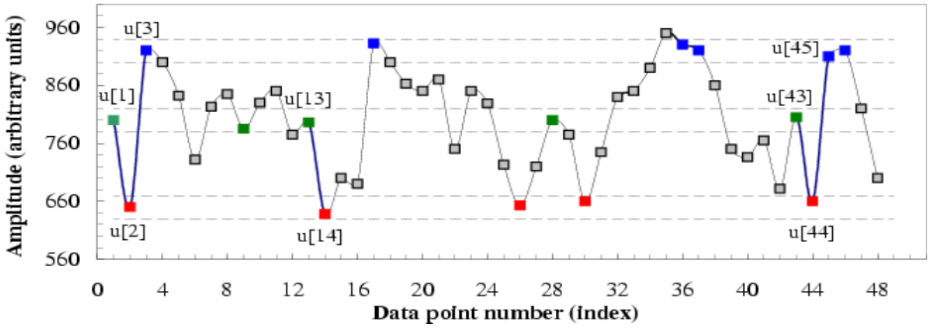

Fig.5. Illustration of the procedure for calculating sample entropy for m=2 and r=20. [16]

3. Finally, the SampEn value of each coarse-grained time series isplotted as function of the scale factor. This plot will reflect the complexity of the signal over the scales, where higher the SamPen value more complex is the time series.

The result of applying the MSE analyses to white and 1/f noise is depicted in Fig.6.

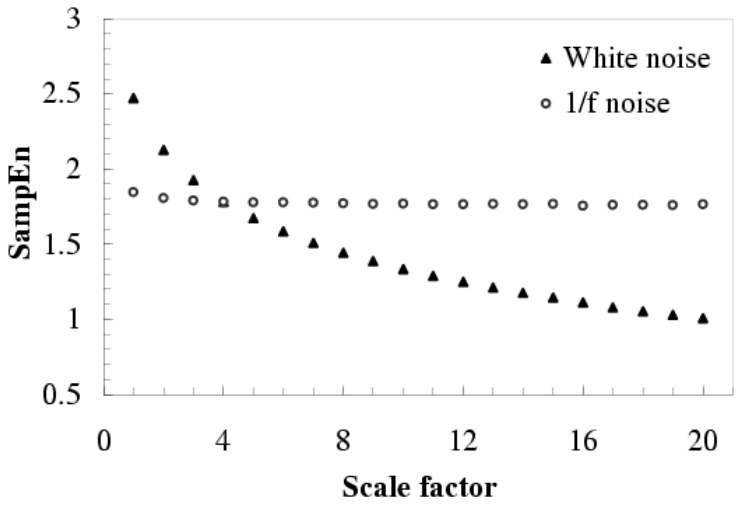

Fig.6. MSE analysis of simulated white and 1/f noise time series, with m = 2, r = 0.15, and N = 30000. Symbols represent mean values over 30 time series. [16]

White noise is an uncorrelated time series and 1/f (also called fractal noise) is a long-range correlated time series [16]. As is shown in Fig.6, white noise has a higher entropy value than 1/f noise for scale 1. However, the entropy value is almost constant for 1/f noise, and monotonically decreases for white noise, such that it becomes smaller than the 1/f noise for scale above 4. This result is consistent with the fact that 1/f contains complex structures across multiple scales, and white noise only contains information on the shortest scale [14]. Thus, the MSE analysis reveals that 1/f is more complex than white noise.

MSE accounts for the fact that complex systems are not perfectly regular neither completely random. Therefore, MSE analysis generally reveals structures with long-range correlations on multiple spatial and temporal scales[18].

2.3 Poincaré plots

The Poincaré plot (PP) is a visual technique used for analyzing long records of physiological data. Since the PP technique summarizes the entire recording and displays nonlinear aspects of the interval sequence, it's easy to recognize patterns and at the same time it's possible to extract information on short and long time behavior of asystem [19]. The PP of RR intervals of healthy and unhealthy subjects has been shown to have a different geometry so it's possible do distinguish them. For these reasons, in the context of medical sciences, this technique is widely used for ascertaining the heart rate variability [5].

The PP technique consists in taking a sequence of intervals and plots each interval against the next interval [19]. Hence, to define the PP for a data vector $x = x_1, x_2, \dots, x_N$ of length N, it's necessary to define two auxiliary vectors [5]:

$$RRi_n = (x_1, x_2, \dots, x_{N-1})$$

$$RRi_{n+1} = (x_2, x_3, \dots, x_N)$$

And finally, plot RRi_{n+1} as function of RRi_n .

2.3.1 RR Interval Poincaré Descriptors

The problem regarding the PP technique use is the lack of quantitative measures that capture the non-linear aspects of the RR interval. Although there are a number of techniques that attempt to quantify the plot's geometric appearance, these methods appear to be insensitive to the nonlinear characteristics of the intervals [19].
One of these techniques uses the standard PP descriptors, SD1 and SD2 [5].

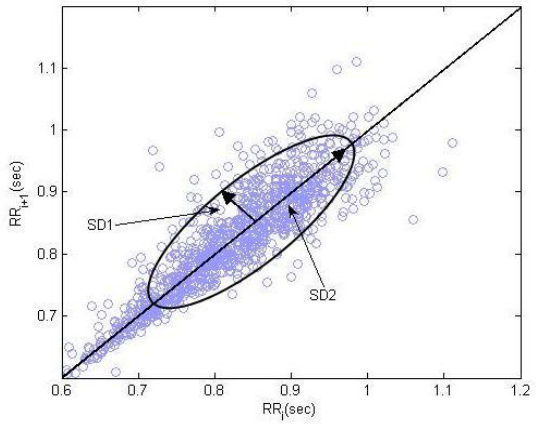

Fig.7. Poincaré plot of RR intervals of a healthy subject. SD1 represents the minor axis and SD2 represents the major axis of the ellipse. [20]

SD1 is the standard deviation of the projection of the PP on the line perpendicular to

to the line of identity (y=-x) and SD2 is the standard deviation of the projection of the PP on the line of identity (y=x) (Fig.7) [5]. Mathematically SD1 and SD2 are defined as [5]:

$$SD1 = \sqrt{Var(x1)}\,, SD2 = \sqrt{Var(x2)}$$

whereVar(x) is the variance of x, and

$$x_1 = \frac{RRi_n - RRi_{n+1}}{\sqrt{2}}\,, x_2 = \frac{RRi_n + RRi_{n+1}}{\sqrt{2}}$$

$x_1$andx_2 correspond to the rotation of RRi_n and RRi_{n+1} by $\theta = \frac{\pi}{4}$[5], respectively:

$$\begin{bmatrix} x_1 \\ x_2 \end{bmatrix} = \begin{bmatrix} cos\frac{\pi}{4} & -sin\frac{\pi}{4} \\ sin\frac{\pi}{4} & cos\frac{\pi}{4} \end{bmatrix} \begin{bmatrix} RRi_n \\ RRi_{n+1} \end{bmatrix}$$

As the SD1 measures the width of the PP, it reflects the short-term variability, and as SD2 measures the length of the PP along the line of identity, it reflects the long-term variability [19]. It is common to draw an ellipse with axes (SD1, SD2) centered on ($\overline{RRi_n}$, $\overline{RRi_{n+1}}$), where the overbar denotes the mean of the vector. This technique is usually called "fitting an ellipse" [5]. However, no actual fitting takes place, the ellipse in only there to help the eye, and a rectangle with sizes (2SD1, 2SD2), might do as well [5]. The total variability measure by the PP is defined by [20]:

$$A = \pi SD1SD2$$

which is the area of the ellipse.

2.3.2 Colored Poincaré Plot

Since the Poincaré Plot of RR intervals has a large number of dots, it's difficult to get a good impression of their distribution in dense areas (Fig.8 (a)). A way to get a better visualization of the PP is to color the dots by density. There is an algorithm to Matlab, *Dscatter* [21], which creates a scatter plot colored by the density of the points. Hot colors, such as brown and red, represent high density areas, i.e., a high concentration of points. Cold colors, such as blue, show the lowest density areas (Fig.8 (b)).

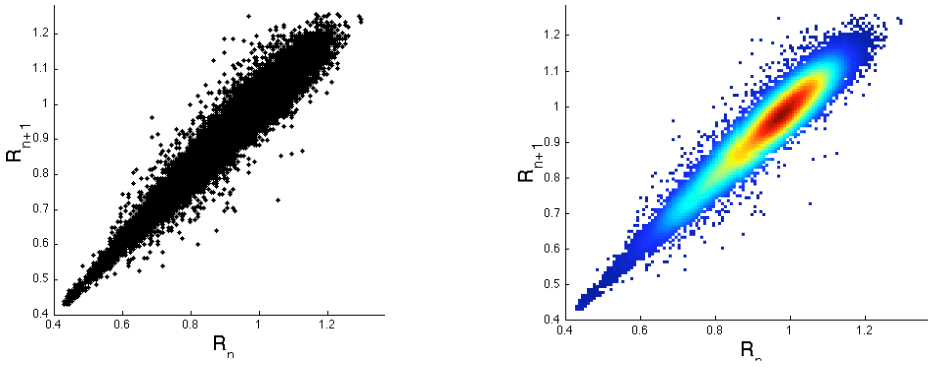

(a)

Fig.8. Poincaré plots of a healthy young subject. (a) A convectional Poincaré Plot. (b) A colored Poincaré plot using *Descatter* algorithm.

2.4 Types of Noise

There are several types of noise-signals, and they are classified based on their statistical properties. The autocorrelation i.e., the internal correlations between successive increments of the signal itself, is one of the properties used to classify the noise-signals. The easiest and more frequently used method to evaluate the autocorrelation is the Power Spectral Density [24]:

$$S(\alpha) \propto \frac{1}{f^{\alpha}}$$

where$f$ is the frequency and α is the scaling exponent. The scaling exponent has values between 0 and 2. $\alpha = 0$means that there are no correlations between successive increments, and $\alpha > 0$ corresponds to sequential dependencies. Two important noises-signals are the white noise and 1/f noise (also called pink or fractal noise). White noise has $\alpha = 0$, thus it has a flat power spectrum reflecting the lack of autocorrelation (Fig.9 (a)), so it represents a random variable [24]. The 1/f noise ($\alpha = 1$) has a power spectrum that is exactly inversely proportional to the frequency (Fig.9 (b)). Thus, this type of noise has long-range correlations [24].

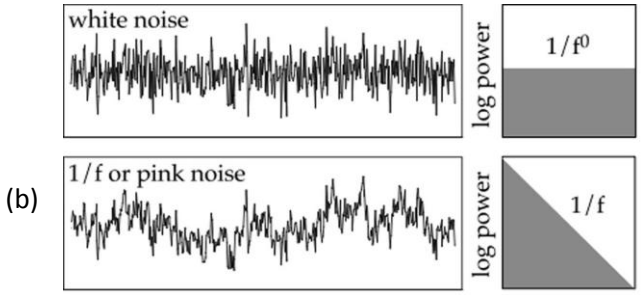

Fig.9. Examples of (a) a white noise time series and its power spectrum representation and (b) a 1/f noise time series and its power spectrum representation.

2.5 Empirical Mode Decomposition

The Empirical Mode Decomposition (EMD) method was specifically developed for decomposing nonlinear, nonstationary signals into their intrinsic frequencies components. The EMD method assumes that any data consists of different simple intrinsic mode oscillations, i.e., EMD method consists in considering oscillatory signals at the level of their local oscillations and iterates on the slow oscillations component as a new signal [25].Each oscillation is referred as an Intrinsic Mode Function (IMF). Typically, the power spectrum of an IMF is a peaked function with predominant power over only a limited range of frequencies. Although, a certain degree of overlap

between the spectrums of consecutive IMFs is expected, different IMFs capture the properties of the original signal on different time scales. Given a signal $x(t)$, the EMD method consists in the following steps[25]:

1. Identify all extrema of $x(t)$, both maxima and minima (Fig.10).

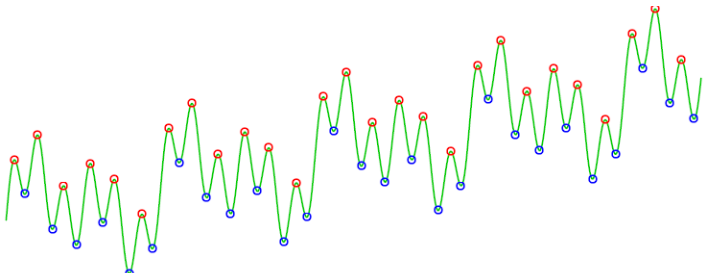

Fig.10. First step of the EMD method: all extrema identifications (red dots are the maxima and the blue dots are the minima). [26]

2. Connect all the local extrema by a cubic spline to form a lower envelope $e_{min}(t)$and upper envelope$e_{max}(t)$(Fig.11).

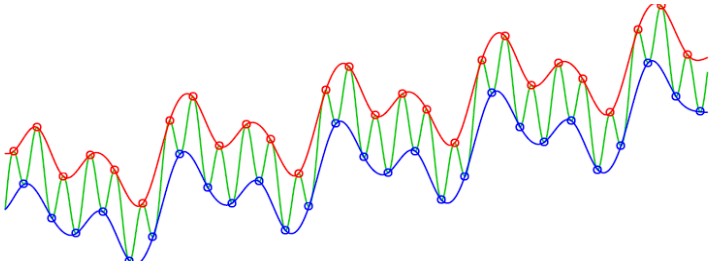

Fig.11. Second step of the EMD method: interpolate between minima and maxima to form a lower and upper envelope, respectively. [26]

3. Compute the average of the envelopes (Fig.12):

$$m(t) = \frac{e_{min}(t) + e_{max}(t)}{2}$$

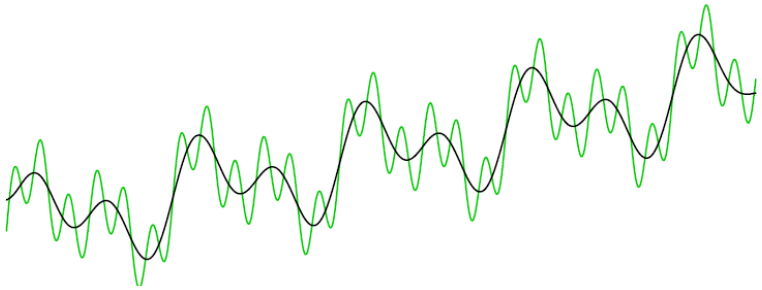

Fig.12. Third step of the EMD method: mean computation of the envelopes. [26]

4. Extract a new series called detail or residues,$d(t)$,that is the difference between the original series $x(t)$ and the mean value of the envelopes $m(t)$, i.e.,:

$$d(t) = x(t) - m(t)$$

In practice, the above procedure has to be refined by a sifting process that consists in repeating all the steps presented previously, until the first IMF is obtained. Therefore, the first IMF, is given by the following k-iterative formula[25]:

$$IMF_1(t) = d_{(k-1)} - m_k(t)$$

An IMF must satisfy the conditions [27]:

a) In the whole data set, the number of extrema and the number of zero crossings must either equal or differ at most by 1;
b) At any time t, the mean value of the "upper envelope" (determined by the local maxima) and the "lower envelope" (determined by the local minima) is zero.

However, it is not always efficient to test for these conditions. Instead, it is recommendedstopping the iterative process when the value of the standard deviation (SD) is below a selected value in the range of (0.2-0.3). The SD is given by the equation [28]:

$$SD = \sum_{t=0}^{T} \left[\frac{[h_i(t) - h_{i-1}(t)]^2}{h_{i-1}^2(t)} \right]$$

In Fig.13, the $IMF_1(t)$, $IMF_7(t)$ and $IMF_{10}(t)$ of the 1/f noise time series is shown.

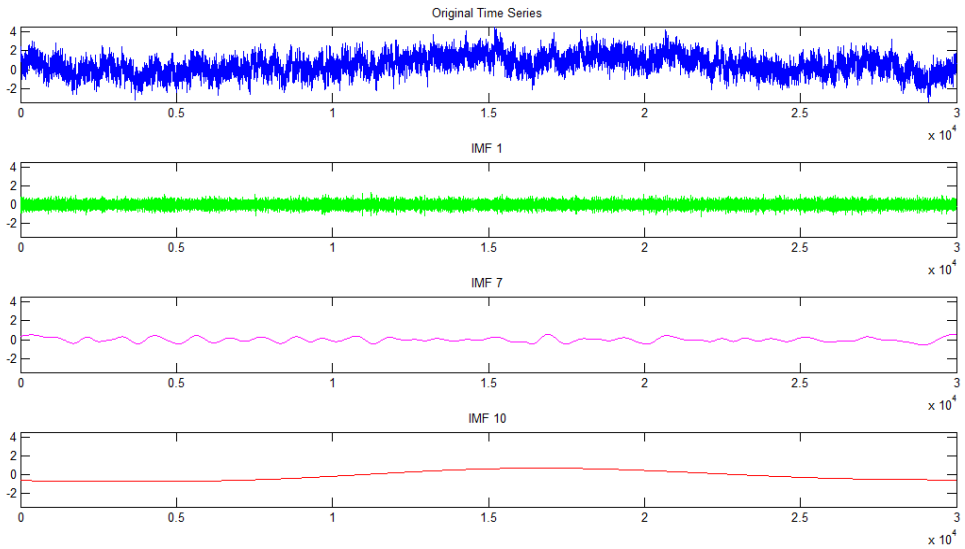

Fig.13. The $IMF_1(t)$, $IMF_7(t)$ and $IMF_{10}(t)$ of the 1/f noise time series, obtained with the EMD method.

Note that if the IMFs are obtained, then the original time series can be reconstructed by [28]:

$$x(t) = \sum_{i=1}^{n} IMF_i(t) + d_n$$

In Fig.14 the summation of the three IMFs represented in Fig.13 ($IMF_1(t)$+$IMF_7(t)$+$IMF_{10}(t)$) is shown. In order to obtain the original time series, the others IMFs components should also be add.

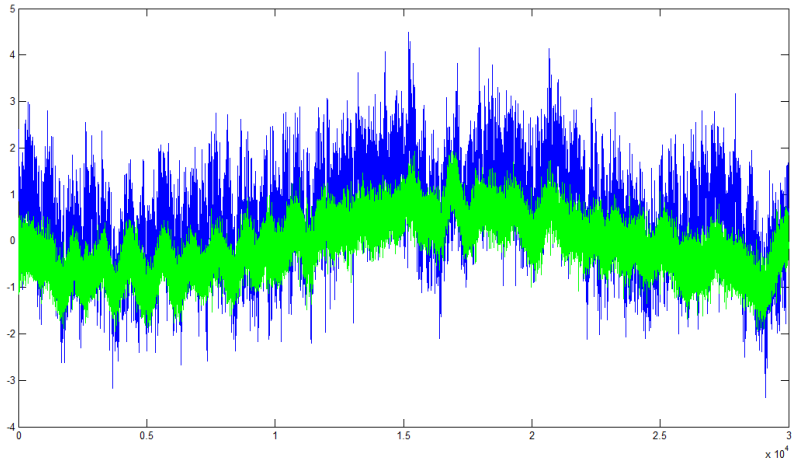

Fig.14. In blue the original time series is represented and in green is represented the summation $IMF_1(t)$+$IMF_7(t)$+$IMF_{10}(t)$.

2.6 Statistical Analysis

Statistical analysis provides a way of quantifying the confidence in the results obtained. However, a statistical test can never prove the truth of a hypothesis, but merely provide evidence to support or refuse it [30]. A common statistical test used in data analysis is the calculation of the P-values, also known as hypothesis test. This type of test is generally used when comparisons are to be made, for example, a characteristic of two different populations. In this chapter, a clarification about the significance of the P-value will be made.

2.6.1 P-Value

The “P” stands for “Probability”, and being a probability, can take any value between 0 and 1. The P-value measures how likely it is that any observed difference of two groups are due to chance [30]. In other words, it is the probability of seeing the observed differences, just by chance if the null hypothesis is true. The null hypothesis is the assertion that the differences observed between two groups are not related and the results are the product of random chance events.If the difference observed between groups are due to random variation, the P-value will be close to 1, but if this difference is unlikely to be due to chance, the P-value will be close to 0 [30].It is common to classify results as statistically significant, based on the P-value being smaller than some specific value, usually 0.05. This value means that the results are only 5% likely to be the result of chance, given that the null hypothesis is true. When the null hypothesis is rejected, the result is assumed to be statistical significant.

3. Materials and Methods

3.1 Materials

On the first part of the project, for the FHR study, 158 FHR tracings were analyzed.These tracings were acquired with a cardiotocograph (CTG) in University of Porto between May 2005 and September 2007. The CTG is a continuous electronic record of the fetal heart rate and uterine activity, obtained via an ultrasound transducer placed on the mother's abdomen[31]. Nine of the 158 FHR tracings are acidemic cases and 149 are healthy cases. Three of the healthy cases were diagnosed as acidemic cases at the time the tracings were acquired. For the analysis of the FHR tracings, these 3 healthy cases, which will be referred as false positive cases,are separate from the others, in order to evaluate the capacity of the algorithms used to correct diagnosed them. All the cases have at least 30 minutes and at maximum 8 hours of data.TheOmniView-SisPorto® software was applied to all the cases in order to obtain the baseline of the FHR. OmniView-SisPorto® is a software developed at the School of Medicine of the University of Porto in collaboration with the Institute of Biomedical Engineering, also in Porto, that analyzes fetal heart rate signals and provides real time alerts to aid intrapartum management [22]. This software is a central monitoring system that provides visual and sound alerts (Fig.15), based on computer analysis of CTG and ST event features [23]. The alerts provide help to the management of labor and the timely todetection of fetal suffering and can be used with existing fetal monitors [23].

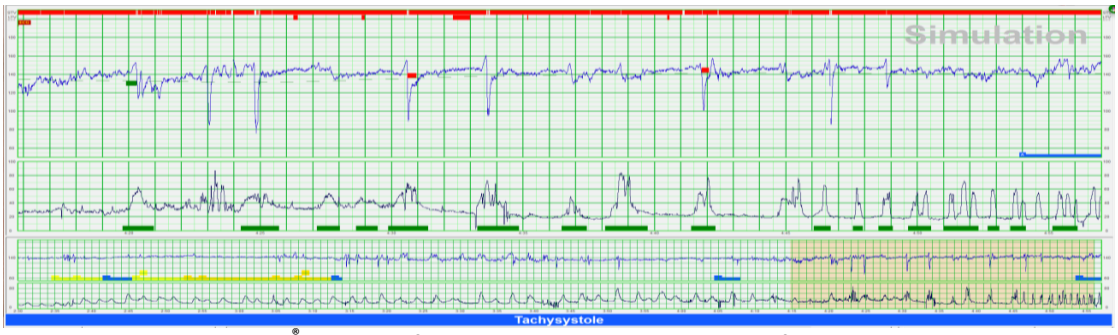

Fig.15. OmniView-SisPorto® user interface. The upper signal represents fetal heart rate and the bottom signal represents uterine contractions. The red line represents deceleration, the green one means accelerations (on fetal heart rate signal) and uterine contractions (on uterine contractions signal) and the blue line represents tachysystole (condition of excessively frequent uterine contractions).

The analysis of the cases was performed offline, and includes estimation of uterine contractions, of fetal heart rate baseline, identification of accelerations, decelerations, and quantification of short- and long-term variability.

Other technique, based on Empirical Mode Decomposition, to obtain the baseline of each case was also used. The compression algorithm Paq8l and MSE analysis was applied to all the cases.

On the second part of the project, Poincaré Maps were used in order to study the HRV. Four healthy old (range 66-75 years), 4 healthy young (range 20-50 years),5 CHF and 4 AF subjects were studied. For further comparison, Poincaré Maps of noise from $\alpha = 0$ to $\alpha = 1$, with a step size of 0.1, were also performed. *Descatter* algorithm was used to colorize the PP. In attempt to quantify the geometry of PP's, fitting an ellipse technique was applied. Finally, the EMD method was also applied in attempting to quantify the HRV of healthy young and healthy old subjects and CHF subjects. This time, there was a distinction between the day and night periods, of the RR intervals of each group. In this case, 26 healthy young subjects (range 20-50 years), 45 healthy elderly subjects (range 66-75 years), and 43 CHF subjects (range 22-78 years), were analyzed.

3.2 Methods

On the first part of the project, for the FHR analyzing, the Paq8l algorithm and MSE were applied. Three procedures were performed:

1. In order to run the compression algorithm, a moving window procedure was applied to the last 30 minutes before delivery. This procedure involved dividing the FHR signal of all the cases, into overlapping windows of 10 minutes with a step size of 1 minute (Fig.16).

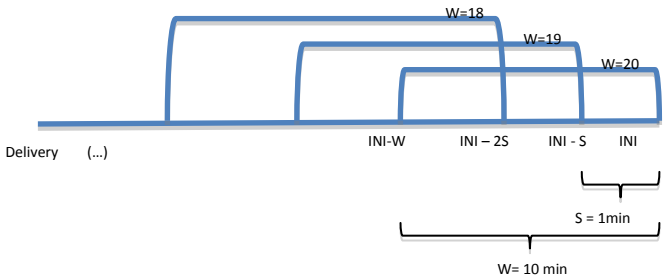

Fig.16. Schematic illustration of the moving window procedure the FHR signal. INI is the initial value (30 minutes), S is the step size (1 minute) and W is the window (intervals of 10 minutes).

This procedure resulted on 20 different intervals and each of them was saved in a file. The Paq8l algorithm was applied to each of these files and the size of the files after compression was plotted as a function of the interval. Note that all the intervals have the same length, so the initial size of each interval is the same for every case. Therefore, it is not necessary to calculate the Compression Ratio.

2. In order to apply the MSE method to the signals, first the OmniView-SisPorto® software was applied for all the cases to obtain the FHR baseline of each case. The baseline was then subtracted from the FHR to *detrended* the signal. *Detrending* was used to remove features that obscure the variable of interest (the complexity of the signal), such as accelerations and decelerations. After the *detrending*, the moving window procedure was applied to the FHR signal. This timethe size of the windows was 20 minutes with a step size of 1 minute. The MSE method was applied to each of these windows for the last 120 minutes before delivery of each case. The complexity index (CI) was calculated trough the summation of the Sample Entropy values from the scale 3 to 6 inclusive, and the CI as a function of the window was plotted.

3. Another method of *detrending* the data, based on EMD method, was also implemented. This time, the aim was to know if there could be detected a difference between healthy and unhealthy fetuses long time after the delivery. In order to do that, the MSE method was applied to the following situations:

    - Last 125 minutes before delivery;
    - Last 60 minutes before delivery;
    - Last 120 minutes before delivery to 60 minutes before delivery.

On the second part of the project, the HRV of healthy young and old subjects and subjects with CHF and AF, were analyzed. The following procedures were performed:

1. Noise from $\alpha = 0$ to $\alpha = 1$ with a step size of 0.1, was coarse-grained from scale 1 to scale 20. In Fig.17 the result of coarse-grained for white and fractal noise, is represented. Then, the multiscale PP of each noise was performed, i.e., the PP of each coarse-grained time series. The *Descatter* algorithm was also used to colorize the PP.

2. The RR intervals of healthy old, healthy young, CHF and AF subjects were coarse-grained from scale 1 to scale 20. The multiscale PP of each subject was performed and the *Descatter* algorithm was also applied to colorize the PP.

3. Geometry quantification of PP was attempted. In order to do that, the ellipse fitting technique was applied. The ratio of area of the PP for scale 20 to area of the PP for scale 1 was calculated for every subject. This value reflects the degree of collapse of the PP from the first scale (scale 1) to the last scale (Scale 20) of the coarse-grained procedure.

4. EMD method was applied in order to study the contribution of each component of the signal for the variability of the heart rate. The EMD algorithm decomposes a signal with N data points into a maximum of $log_2 N$ intrinsic mode functions (IMFs). For the time series analyzed here we typically obtain 10 components with characteristic frequencies given by sample frequency/(2n+1), where $1 \leq n \leq 10$. The first 5 IMFs have predominant power for frequencies ranging from approximately 1 to 30 Hz, and the last 5 IMFs have predominant power for frequencies ranging from approximately 0.05 to 1 Hz. The HRV of all the subjects during the day and night periods was compared. Twenty-six healthy young cases, 45 healthy old cases and 43 CHF cases were analyzed. The value of the standard deviation of each IMF component, from 1 to 10, divided by the standard deviation of the original times series was calculated. This value was obtained for each case, and then the average of healthy old, healthy young and CHF groups were calculated. Finally, the average value of each group as a function of the IMF component was plotted.The p-value was calculated in order to evaluate the statistical significance of the results. This procedure was also applied for a white and a fractal noise time series to further comparison.

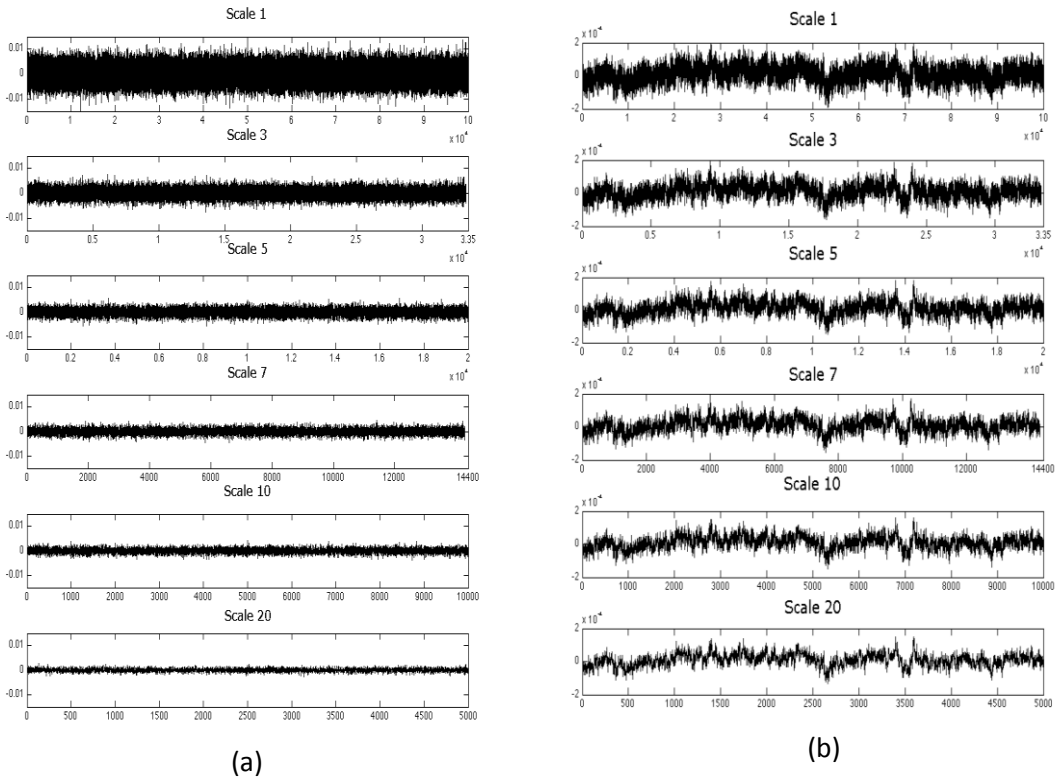

Fig.17. Result of coarse-grained procedure. In the figure is only represented scale 1,3,5,10 and 20. (a) White Noise ($\alpha = 0$); (b) Fractal Noise ($\alpha = 1$).

4. Results

4.1 FHR Analysis

In Fig.18 the intervals' sizes (in bytes) after applying the compression algorithm Paq8l, are shown. The green lines represent the healthy fetuses. The black lines are the fetuses diagnosed with acidemia and the blue lines are false positives (healthy cases diagnosed as acidemic cases).

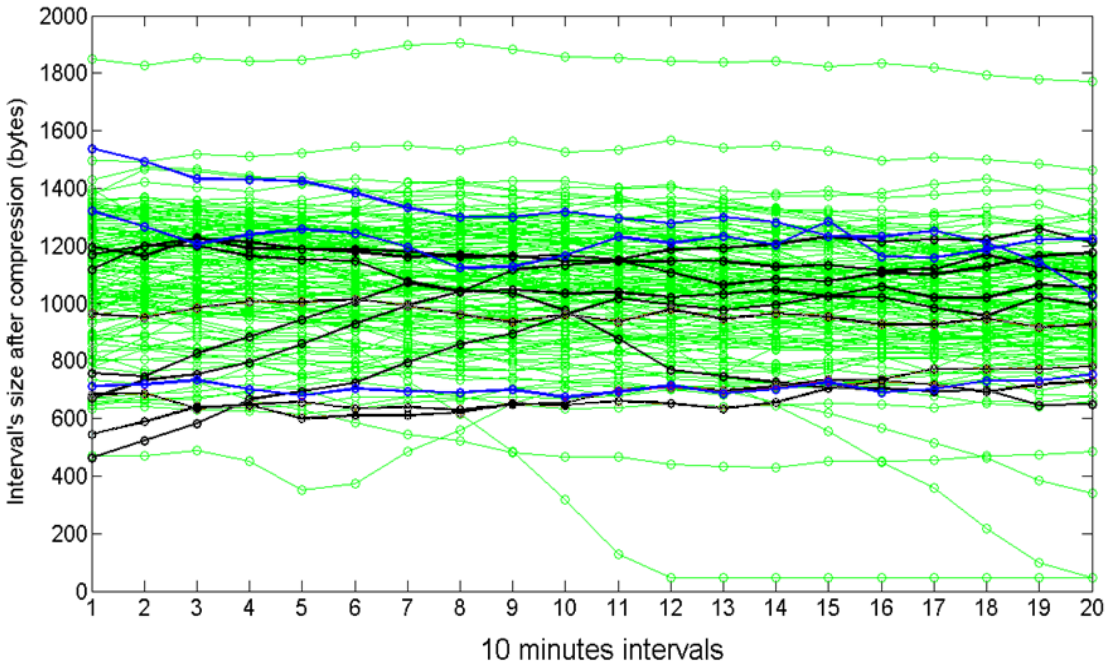

Fig.18. Size of the files (each file contained a different interval) after compression. The green lines are healthy cases, black lines represent acidemic cases and blue lines are false positive cases. The interval 20 ($x = 20$) contains 30 minutes to 20 minutes of FHR signal and the interval 1 ($x = 1$) contains the last 10 minutes of the FHR signal before delivery.

In Fig.19 the complexity index of intervals of 20 minutes, of the 120 last minutes before delivery, is represented. In this case, the FHR signals were *detrend* with the baseline obtained with the OmniView-SisPorto® program. The green lines are the healthy cases, the black lines represent acidemic cases and the blue lines are false positive cases. Some cases are missing in this plot (1 false positive and some acidemic cases), since they didn't have enough data points to be plotted (they had less than 120 minutes of data).

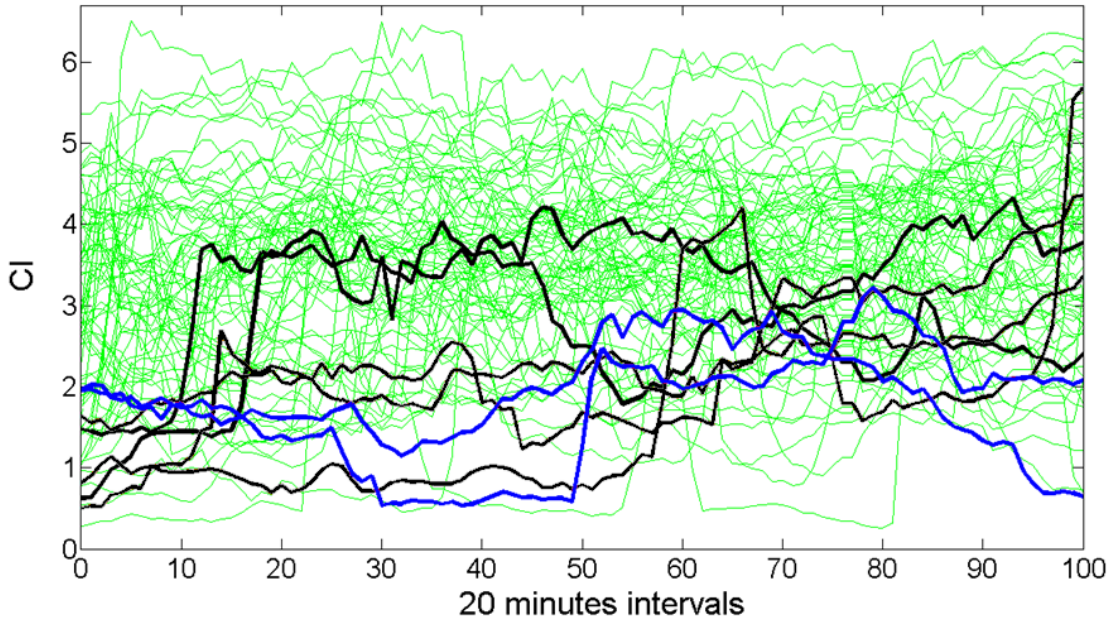

Fig.19. Complexity index of each interval (each interval has 20 minutes) 120 minutes before delivery. The green lines are healthy cases, black lines represent acidemic cases and blue lines are false positive cases. At X-axis, 100 represents the interval of 120 minutes to 100 minutes before delivery and 0 represents the 20 last minutes before delivery.

In Fig.20 the MSE analysis of the last 125 minutes of each case is presented.The green lines are healthy cases, black lines are acidemic cases and blue lines are false positive cases. This time, the FHR signals were *detrend* with the EMD method.

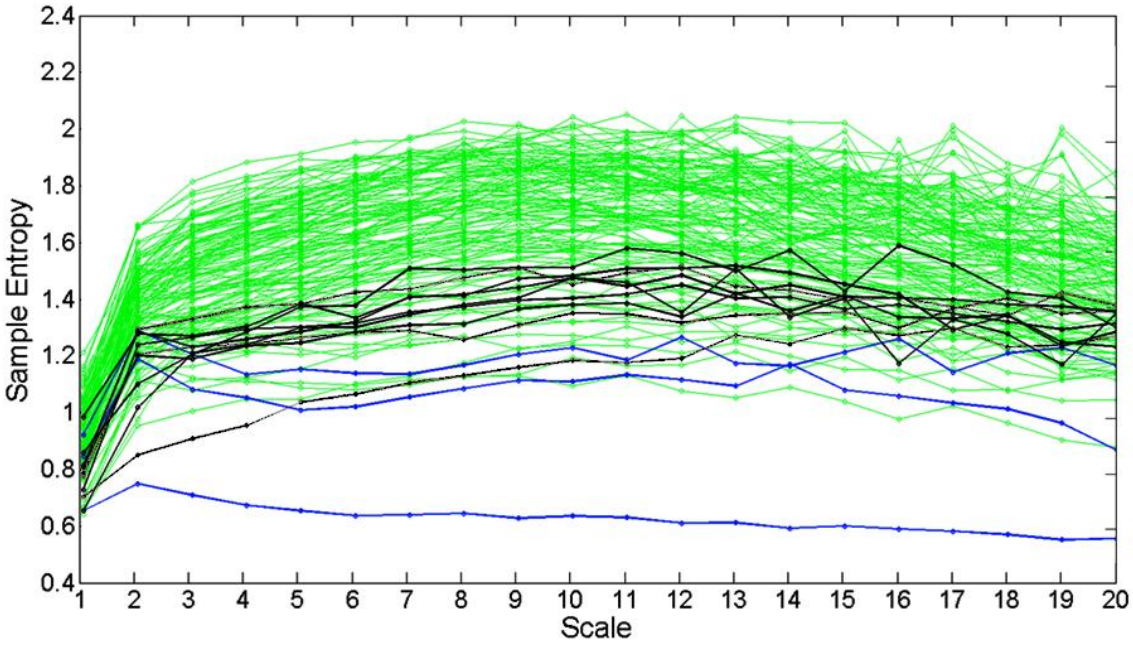

Fig.20.MSE analysis of the last 125 minutes before delivery. The green lines are healthy cases, black lines are acidemic cases and blue lines are false positive cases.

In Fig.21 the MSE analysis of the last hour before delivery of the FHR signal, for all cases, is shown. As in the previous plot, the green lines correspond to healthy cases, black lines are acidemic cases and blue lines are false positive cases.

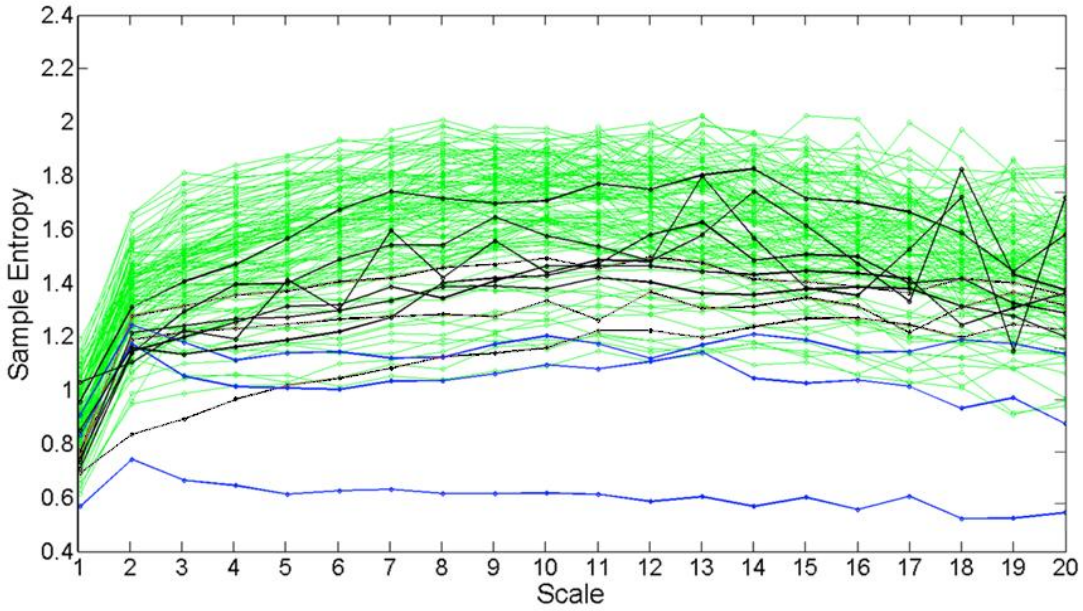

Fig.21.MSE analysis of the last hour before delivery. The green lines are healthy cases, black lines are acidemic cases and blue lines are false positive cases.

In Fig.22 the MSE analysis of the interval between thelast hour before delivery and two hours before delivery of the FHR of all cases, is present. The green lines are healthy cases, black lines are acidemic cases and the blue line is a false positive case. Some of the cases are not represented, since they had not enough data points to apply the MSE method.

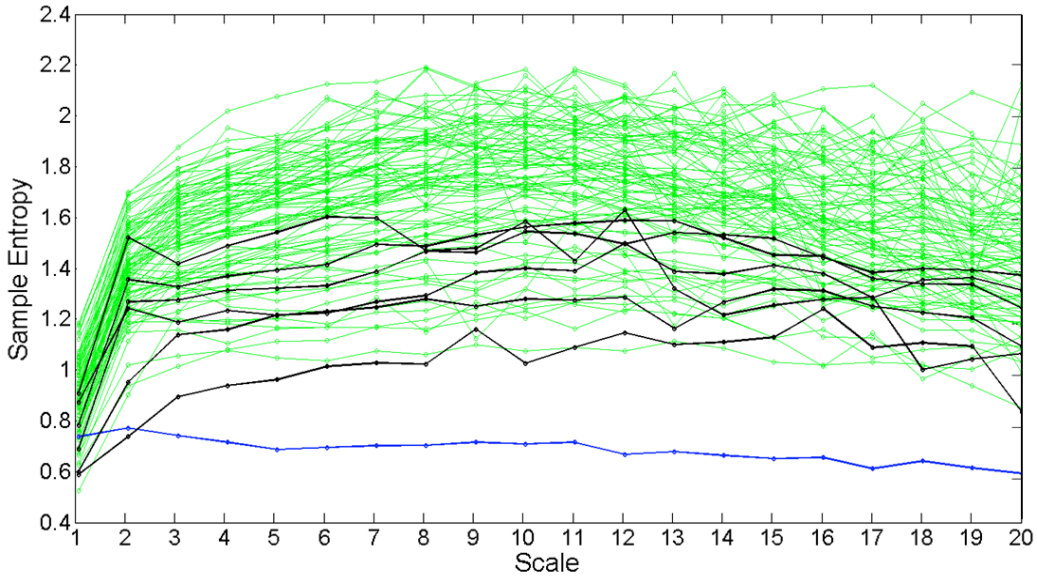

Fig.22. MSE analysis of the 2 hours before delivery to the last hour before delivery. The green lines are healthy cases, black lines are acidemic cases and the blue line is a false positive case.

4.2 HRV Analysis

In Fig.23 the multiscale PP (the PP of the coarse-grained time series) of white noise and 1/f noise is presented. There are only 4 scales plotted, just to perceive the evolution of the geometry of the PP across the scales.

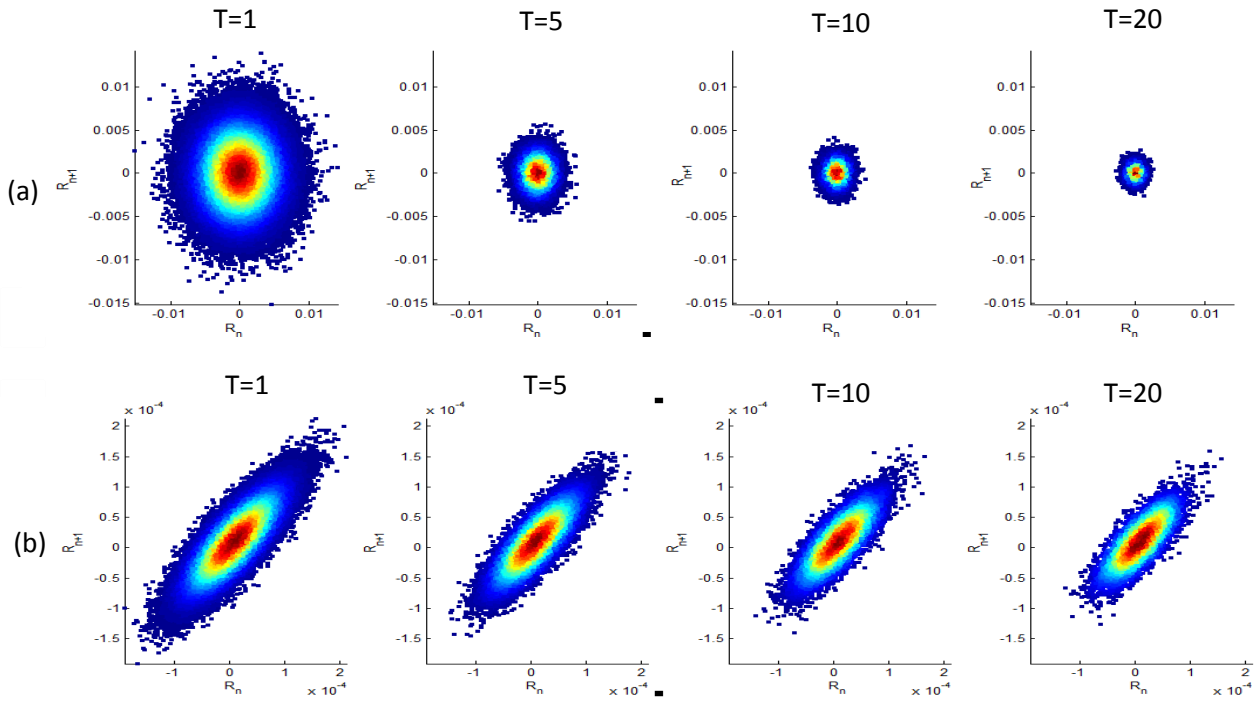

Fig.23 Poincaré plot of the coarse-grained time series for scales T=1,T=5,T=10 and T=20, of (a) White noise ($\alpha = 0$); (b) 1/f noise ($\alpha = 1$).

In Fig.24 is shown the multiscale PP of two healthy young subjects and in Fig.25 is presented the multiscale PP of two old subjects.

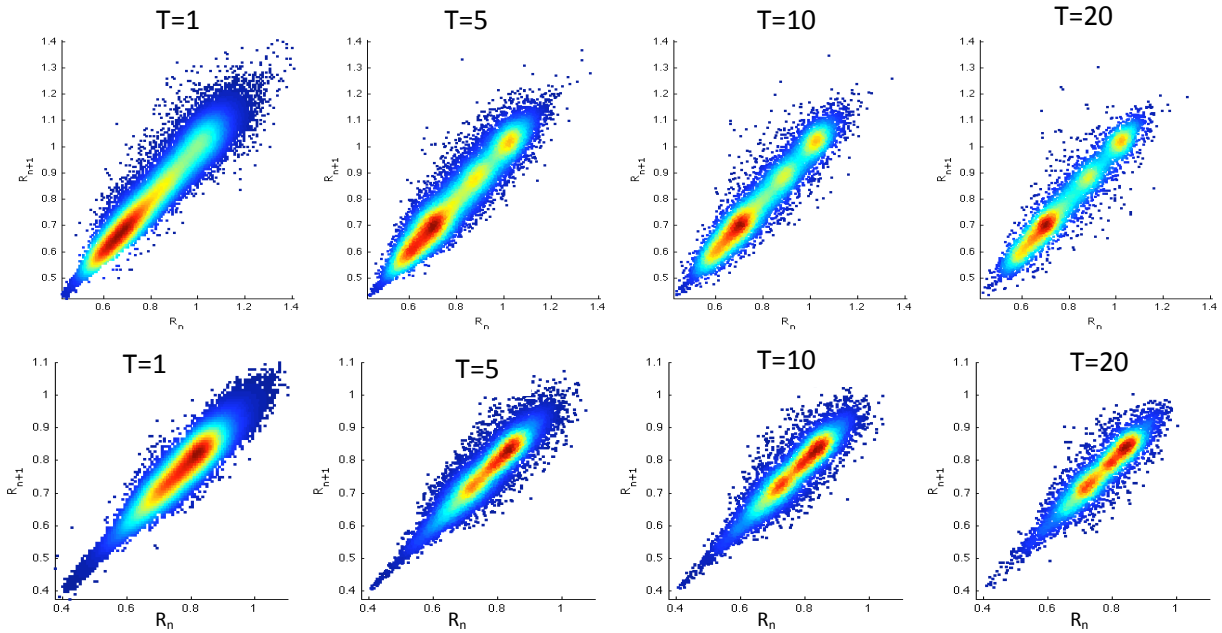

Fig.24. Multiscale PP of two different healthy young subjects. There are only 4 scales (T=1, T=5, T=10 and T=20) represented.

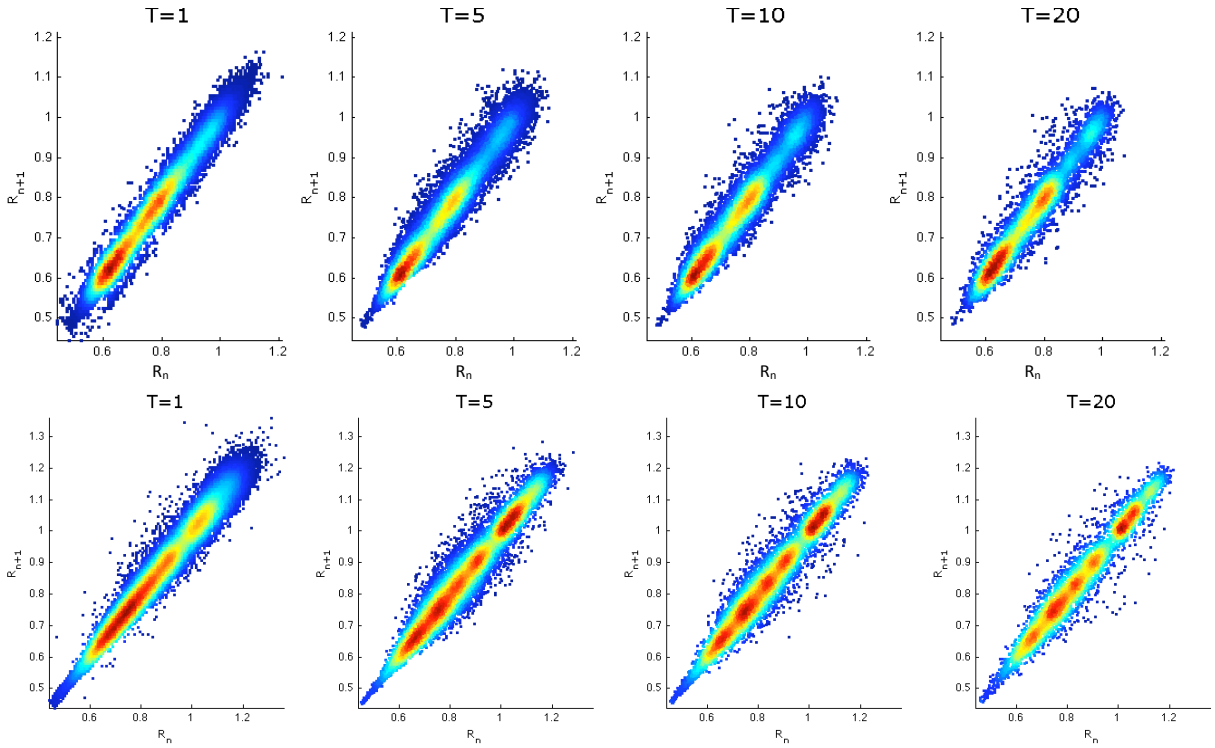

Fig.25. Multiscale PP of two different healthy old subjects. There are only 4 scales (T=1, T=5, T=10 and T=20) represented.

In Fig.26 is shown the multiscale PP of two CHF subjects and in Fig.27 is presented the multiscale PP of two AF subjects.

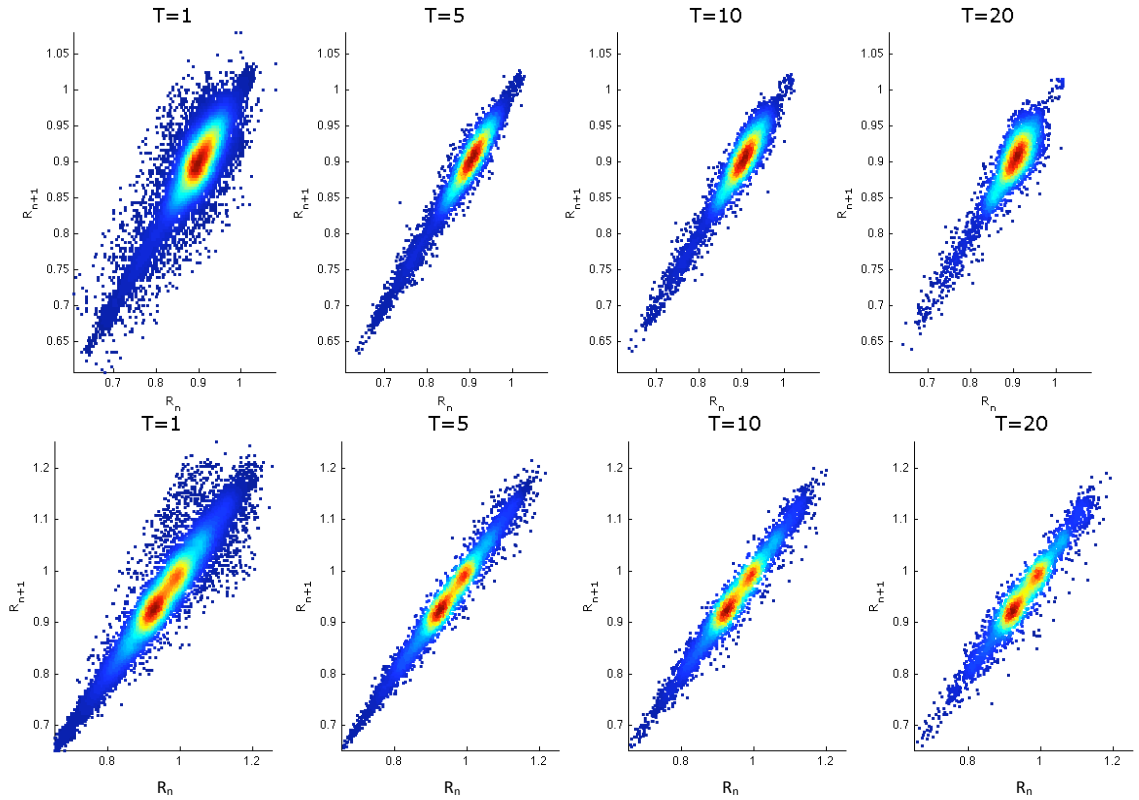

Fig.26. Multiscale PP of two different CHF subjects. There are only 4 scales (T=1, T=5, T=10 and T=20) represented.

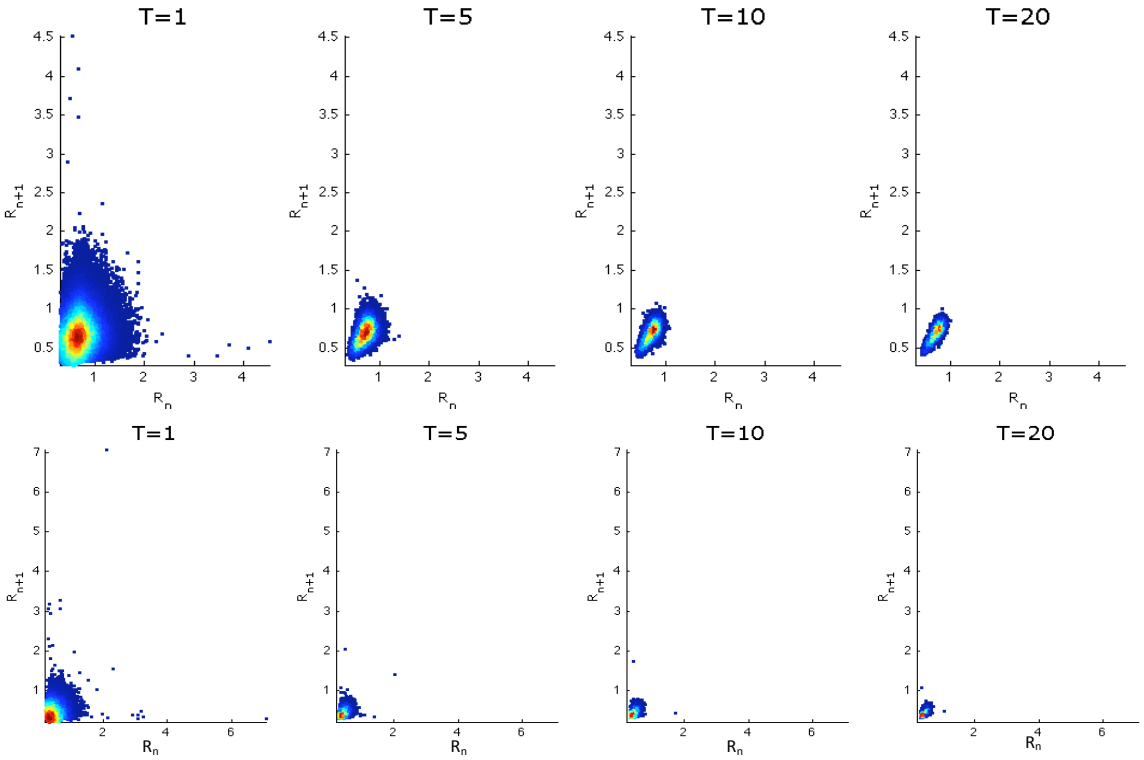

Fig.27. Multiscale PP of two different subjects with AF. There are only 4 scales (T=1, T=5, T=10 and T=20) represented.

The Fig.28 shows the ratio of areas (the area of the PP of scale 20 divided by the area of the PP of scale 1) of healthy young and old, CHF and AF subjects.

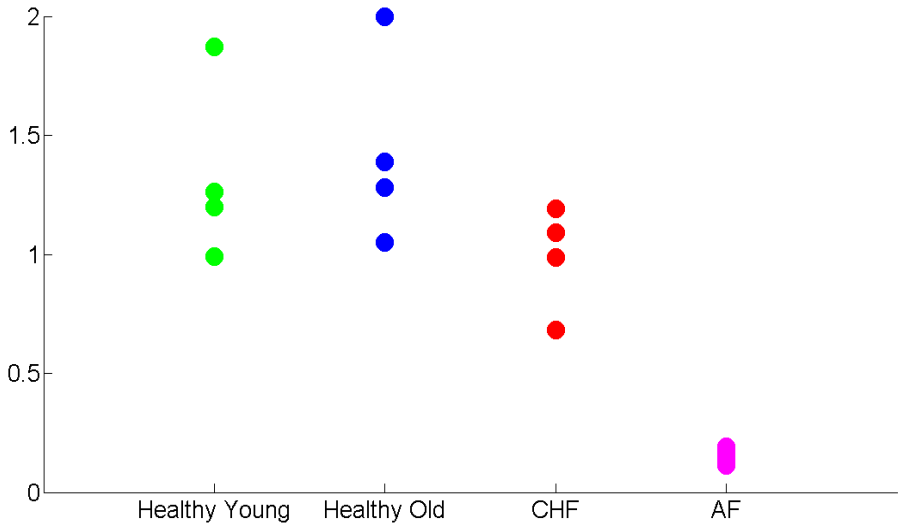

Fig.28. Ratio of areas of healthy young (green dots), healthy old (blue dots), CHF (red dots) and AF (magenta dots) subjects.

In Fig.29, the value of the standard deviation of each IMF component divided by the standard deviation of the original times series, for white and fractal noise, is presented.

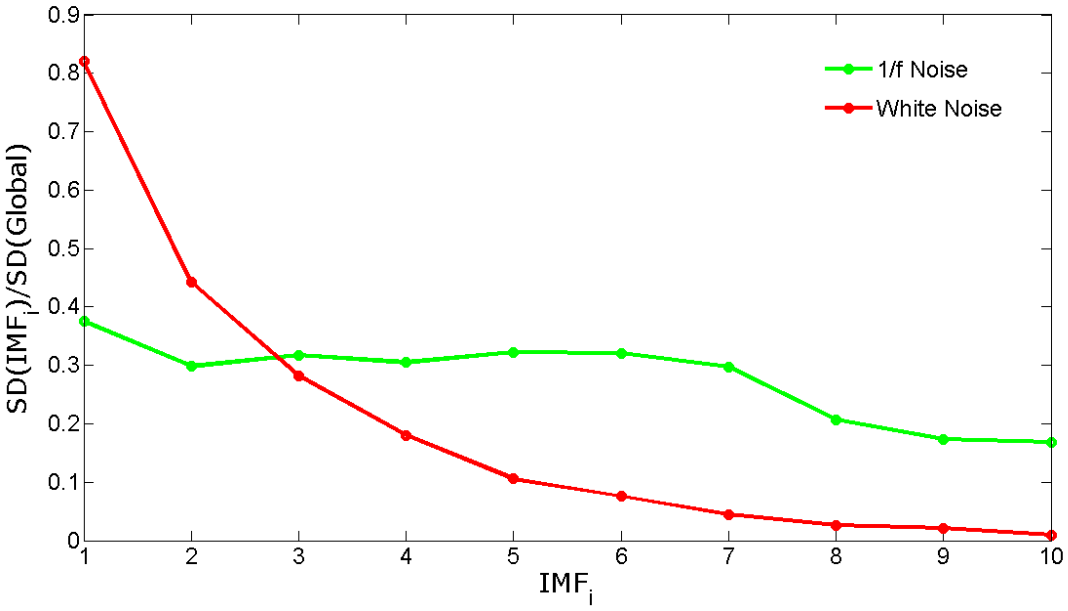

Fig.29. The value of the standard deviation of each IMF component divided by the standard deviation of the original times series, for white (green line) and fractal noise (red line).

The value of the standard deviation of each IMF component of RR interval divided by the standard deviation of the original times series, for healthy young and old, and CHF subjects, for the day and night periods are shown in Fig.30(a) and in Fig.30 (b), respectively.

For the day period, the difference between the healthy young and the healthy old and the CHF group for all the IMF's, except forIMF_7, is statistical significant (P-value < 0.03). However, the difference between the healthy old and the CHF subjects doesn't exhibit statistical differences (P-value > 0.05).

For the night period, the difference between the healthy young and healthy old group isn't statistical significant (P-value > 0.05). Though, the difference is significant between the healthy and the CHF group (P-value < 0.04) expect for the IMF_4 ,IMF_5, IMF_6 and IMF_{10}.

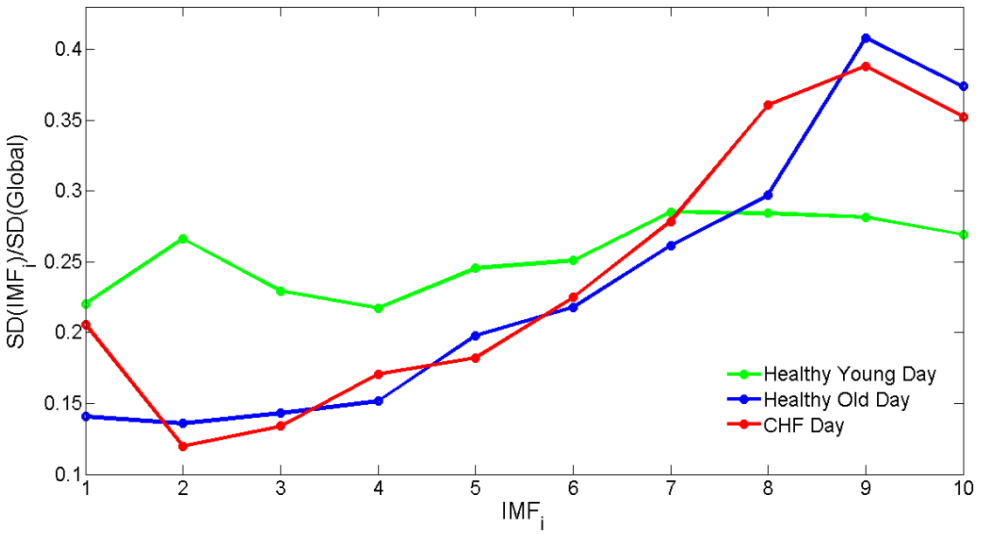

(a)

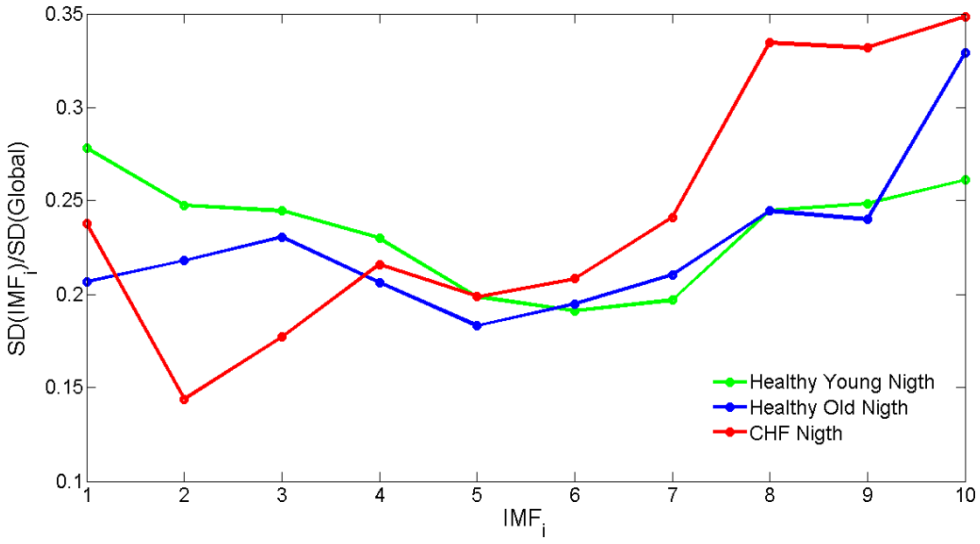

(b)

Fig.30. The value of SD of each IMF component of RR interval divided by the SD of the original time series, for healthy young (green line), healthy old (blue line) and CHF (red line) groups, during the (a) day period and (b) night period.

The comparison between the day and night periods for each group is presented in Fig.31.

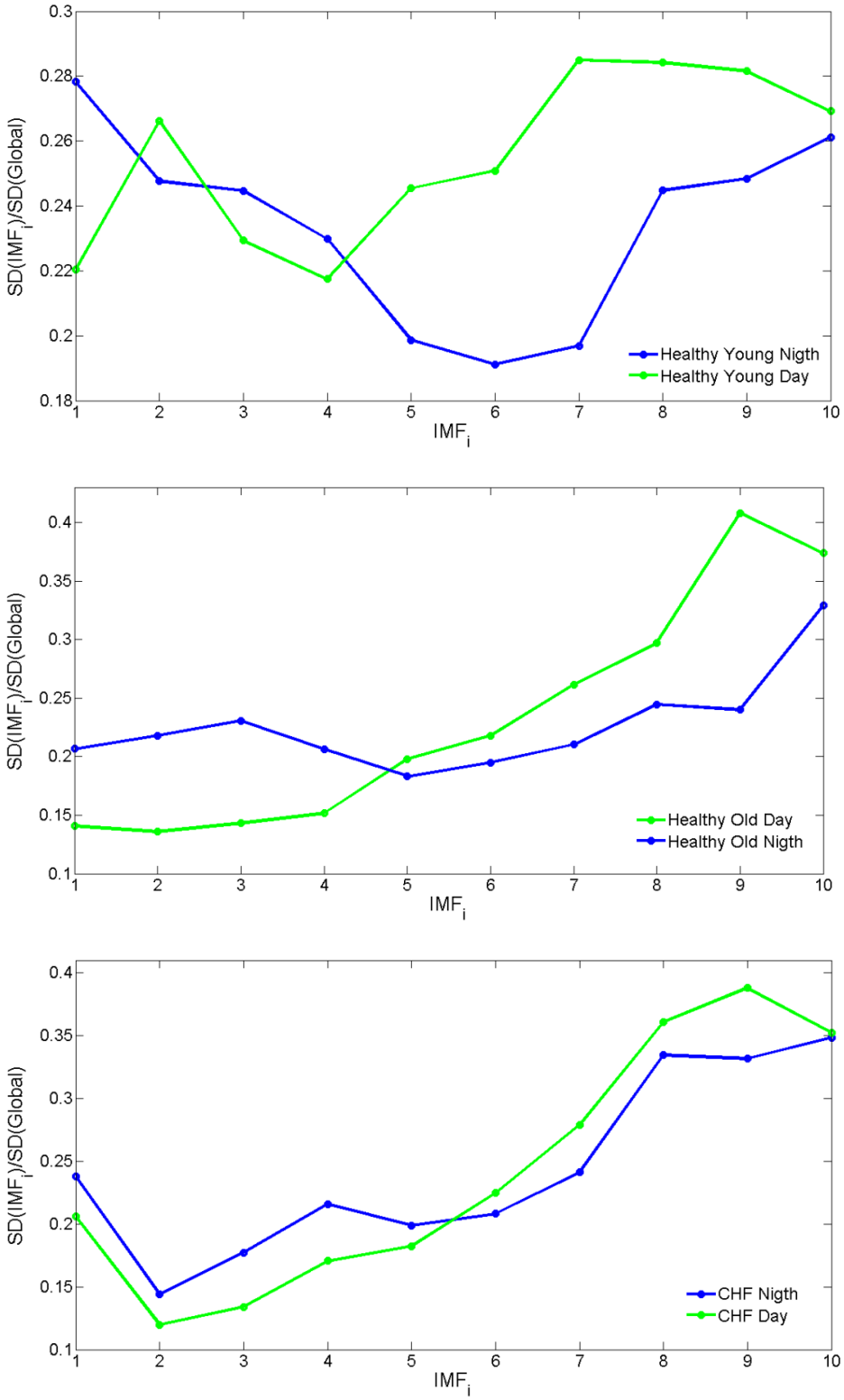

Fig.31. The value of the SD of each IMF component of RR intervals divided by the SD deviation of the original time series, for the day period (green lines) and night period (blue lines), for (a) healthy young, (b) healthy old and (c) CHF group.

5. Discussion

Although there was perceived a difference between some healthy and acidemic fetuses, the Paq8l algorithm didn't have success on separating all the healthy cases from the unhealthy cases. Since the compression algorithms are based on the information theory, which states that simple sequences can be described concisely and complex sequences cannot, these types of algorithms assume that completely random signals are much more complex than the constant ones, which it's proved not to be true. Therefore, the compression-based algorithms don't account for the fact that complex systems are not perfectly regular neither completely random, which explains why the Paq8l algorithm failed to separate some acidemic cases from the healthy ones.

The MSE analysis for the 20 minutes interval, within the 120 last minutes before delivery, proved to be very effective on separating the acidemic cases from the healthy cases, 30 minutes before delivery. On this interval of time, the complexity indexes of acidemic cases are much lower than the complexity index of healthy cases. Even the false positive cases have a complexity index higher than acidemic cases 30 minutes before delivery, which makes sense, since the false positive cases are true healthy cases. Thus the MSE analysis revealed that the acidemic cases suffered a loss of complexity close to delivery, whereas the healthy cases preserved their high complexity along the time.

Applying the MSE analysis for the 125 minutes before the delivery showed a significant separation between healthy and acidemic cases. Most of the healthy cases have an entropy value higher than the unhealthy ones, which suggest that the healthy cases are more complex than the acidemic cases, which was the initial hypothesis. However, the false positive cases have an entropy value lower than the most of the acidemic cases. Moreover, one of these false positive cases exhibits no complexity at all.

Considering the plot of the MSE analysis of the last hour before delivery, it is shown almost the same separation between healthy and acidemic cases as in the previous plot. However, one of the acidemic cases exhibits a very high entropy value and two other acidemic cases show some oscillations on the entropy value along the scales. Curiously, in the plot shown the MSE analysis for the interval of time between two hours before delivery to one hour before delivery, these oscillations in the entropy value disappear. In addition to that, the acidemic case that exhibited a high entropy value in the previous plot, appeared to have a lower entropy value than the most of the acidemic cases. It is also noticeable that the some acidemic cases with low entropy value two hours before delivery improve their condition and have entropy values

similar to the healthy cases one hour before delivery. This apparent improvement of healthy condition can be explained by the pre-processing of the FHR signal, such as noise contained by the signal and the baseline used in *detrending* not fitting perfectly the signal. Besides that, the intervals created by the moving window procedure didn't have all the exact same size. This happened because the length of the FHR signal of each case is different, and the algorithm created for the moving window procedure, eliminated the portions of the FHR that contains no signal (segments of the FHR that equals to 0). This finding is very important since it alerts for the fact that in medical diagnosis, the quantity of data that is used is essential to make a correct diagnosis. To use few data points could yield to wrong conclusions about the healthy status of a system.

The PP of the white noise shows a collapse of the area along the scales. This reflects the fact that the white noise only contains information on the shortest scale On the other hand, the PP of the fractal noise exhibits always the same pattern and size along the scales. This plot reflects the complex structures contained by the 1/f noise across multiple time scales. The PPs of the healthy young subject's exhibit a comet-like shape. The loss of density of the points is the only thing that appears to slightly change, and it's due to the coarse-grained procedure, which results in lesser points for higher scales. Thus, the PP reflects the fractal nature of the healthy biologic systems. Its behavior can be compared with the 1/f noise's PP, which contains information across multiple scales. The PPs of healthy old subject's exhibit also a comet-like shape, but thinner than the PPs of the healthy young subjects. The PP's don't appear to change across the scales, except the density of points for the reasons discussed above. The PPs of the CHF subjects have a different shape, comparing with the healthy subjects. Moreover, the geometry of the PP's slightly changes across the scales. The PP's of the AF subjects have a very different shape from the other subjects' PPs. It looks like a quarter of a sphere at scale 1, and then its area decreases across the scales. This behavior is very similar to white noise's PP behavior. These results confirm the hypotheses that healthy systems contain information across multiple scales thus they are more complex than subjects with diseases, which only exhibit information on the shortest scale.

The attempt to quantify the degree of collapse of the PP for each subject shows some inconsistencies. For example, one of the healthy old cases appeared to increase 2 times the area between the first scale and the last. However, if we examined the PP of this case, we cannot see this area's expansion. These results lead to the conclusion that the fitting ellipse technique has strong limitations. The primary limitation of using this technique to quantify the geometry of the PP's, is that standard descriptors SD1 and SD2 are linear statistics and hence the measures do not directly quantify the nonlinear aspect of the time series contained in the plot. Consequently, this technique proved not to be very efficient.

Finally, another method to quantify the HRV was used, based on the EMD method. In the case of 1/f noise all IMFs (low and high frequency) contribute equally to the original signal. That means that the SD of the IMF of high frequency is equal to the SD of the IMF of low frequency. In contrast, for white noise the IMF component that contributes the most to the signal is the one with the highest frequency. The SD of low frequency IMFs is very low for white noise. These results are consistent with the fact of 1/f noise being a fractal signal (carrying information on multiple time scales) while white noise is not.

The EMD method revealed that the SDs of high-frequency IMFs were higher for young healthy than for elderly healthy subjects and CHF patients, both during the day and night. These results imply that the amplitude of the fluctuations on short time scales is larger for healthy young than for both elderly and CHF patients and is consistent with the described overall loss of heart rate variability with aging and disease. In addition, these results show that the SDs of low-frequency IMFs were higher for CHF patients than for elderly and young healthy subjects. These results reinforce the fact that the HR dynamics of CHF patients is dominated by slow oscillation trends and not high frequency variability. From a physiologic point of view these results suggest a breakdown of the neuroautomonic control mechanisms in CHF patients.

The profile of the day and night curves for the healthy young group are qualitatively different from each other. In the case of the healthy old group, there is also a differencebetween the curves but it's not as accentuated as the healthy young group. However, for subjects with CHF there is not a significant change in the curve's profile. Therefore, the differences between the day and night dynamics of subjects with heart diseases are less marked than for healthy subjects. This fact is related with the loss of adaptive capacity.

6. Conclusion

In the pratical approach of this project, the compression-based algorithm used to quantify the complexity of physiological data proved not to be very efficient. In the other hand, the MSE method along with moving window procedure allowed to separate the acidemic cases from the healthy cases. Although there wasn't a perfect separation between the two groups, it is possible to create a confidence interval, where all the cases that are in that interval have a high probability to be a healthy fetus, and if they are out, they have a change to have acidemia. Besides that, a more accurate pre-processing applied to the signals and cases with more data points might improve these results.

In the theoretical approach of this project, the Poincaré Maps applied to the coarse-grained time series of healthy and diseased subjects, demonstrated that the initial hypotheses were true, i.e., they showed that the behavior of the geometry of the PP over the scales of healthy subjects was close to the behavior of the 1/f noise. It also demonstrated that the AF subjects have a behavior similar to white noise in these plots. As we can tell, these Poincaré Maps applied to the coarse-grained time series were never used before. Even though the PP proved to be a very powerful visual technique, where it is possible to evaluate the variability of different groups and distinguished them by just visual inspection, it would also be interesting if it was possible to quantify the geometry of the PPs. The fitting ellipse technique proved to have a lot of limitations. Although the EMD method proved to be very effective on characterizing the variability of each group, it is not a direct quantification of PP's geometry.

Concluding, the practical approach of this project demonstrated that the multiscale entropy analysis along with moving window procedures can be a very effective method of evaluating the healthy status of a fetus based on the FHR. This is important, because the development of an efficient algorithm that analyzes the FHR and gives accurate information about the healthy status of the fetuses would be very useful in labor management. It would help diagnosing intrapartum complications, proving a faster and a better intervention. The theoretical approach of this project demonstrated that the HRV analysis using PPs in multiscale is a very interesting approach, as it is a visual technique that shows the fractal nature of the HRV and the loss of variability in the subjects with heart diseases. A quantitative measure of the geometry of the PPs that accounts for the nonlinearities is also an interesting topic for further investigation.

References

[1] Wyss Institute for Biologically Inspired Engineering. URL: http://wyss.harvard.edu/

[2] Harvard Medical School Portugal Program. URL: http://www.hmsportugal.pt/

[3] M. Jonsson, S. Nordén-Lindeberg, I Ostlund, U Hanson, *Metabolic acidosis at birth and suboptimal care – illustration of the gap between knowledge and clinical practice,* BJOG - An International Journal of Obstetrics and Gynecology, 2009

[4] R. K. Freeman, T. J. Garite , M. P. Nageotte, *Fetal Heart Rate Monitoring,* Lippincott Williams &Wilkins, 4th edition, 2012

[5] J. Piskorski, P. Guzik, *Filtering Poincaré Plots*, Computational Methods in Science and Technology 11(1), 39-48, 2005

[6] C.-K. Peng, M. Costa, A. L. Goldberger, *Adaptive Data analysis of complex fluctuations in physiologic time series*, World Scientific Publishing Company, vol. 1, 2009.

[7] Akay, Metin, "Electrocardiography", *Encyclopedia of Biomedical Engineering*, Vol.6 Wiley, 2006

[8]Maj Maria J. De Jong, David C. Randall,*Heart Rate Variability*, Journal of cardiovascular Nursing, Vol. 20, No. 3, 2005

[9] John D. Keith, *Congestive Heart Failure*, Pediatrics Vol. 18 No. 3, 1956

[10] Akay, Metin, "Atrial Fibrillation", *Encyclopedia of Biomedical Engineering*, Vol.6 Wiley, 2006

[11]M.Costa, A. L. Goldberger , C.-K. Peng, *Multiscale Entropy Analysis (MSE),* Beth Israel Deaconess Medical Center, Boston, USA

[12]PhysioNet Tutorials, "Complexity vs Variability". URL: http://www.physionet.org/tutorials/cv/

[13] Matt Mahoney, Data compression programs. URL: http://cs.fit.edu/~mmahoney/compression/

[14] M. Costa, A.L. Goldberber, C.-K.Peng,,*Multiscale Entropy Analysis of Complex Physiologic Time Series,* PhysicalReviewLetters, Vol. 89 No 6, 2002

[15] M. Costa, A.L. Goldberber, C.-K.Peng,,*Multiscale Entropy to Distinguish Physiologic and Synthetic RR Time Series*, Beth Israel Deaconess Medical Center, Boston, USA

[16] PhysioNet Tutorials, "Multiscale Entropy Analysis (MSE)". URL: http://www.physionet.org/physiotools/mse/tutorial/

[17] J. S. Richman, J. R. Moorman, *Physiological time-series analysis using approximate entropy and sample entropy*, American Journal of Physiology - Heart and Circulatory Physiology, Vol278, 2000

[18] M. Costa, A.L. Goldberber, C.-K.Peng, *Mutiscale entropy analysis of biological signals*, Physical Review E, 2005

[19] M. Brennan, M.Palaniswami, P. Kamen, *Do Existing Measures of Poincaré Plot Geometry Reflect Nonlinear Features of Heart Rate Variability?*, IEEE Transactions on Biomedical Engineering, Vol. 48, No. 11, 2001

[20] C.K. Karmarkar, A. h. Khandoker, J. Gubbi, M. Palaniswami, Complex Correlation Measure: *a novel descriptor for Poincaré Plot*, BioMedical Engeneering OnLine 8:17, 2009

[21] Matlab code of dscatter.m function is available as a part of "Flow Cytometry Data Reader and Visualization" toolbox at Matlab Central file exchange (accessed July 13,2012) URL: www.mathworks.com/matlabcentral/fileexchange/8430-flow-cytometry-data-reader-and-visualization

[22] The SisPorto Project. URL: http://sisporto.med.up.pt

[23] OminiView-SisPorto. URL: http://www.omniview.eu/

[24]David L. Gilden, *CognitiveEmissionsof 1/f Noise*, PsychologicalReview, Vol 108(1), 2001

[25] J. McGonigle,M. Mirmehdi, A. L. Malizia*, Empirical Mode Decomposition in data-driven fMRI analysis*, Universityof*Bristol1s t ICPR Workshop on Brain Decoding, 2010*

[26]P. Flandrin, P. Gonçalves, G. Rilling, *Detrending and Denoising with Empirical Mode Decompositions*, XII European Signal Processing Conference, 2004

[27] Vesselin Vatchev, *The analysis of the Empirical Mode Decomposition Method*, USC,2002

[28] H. Khatri, K. Ranney, K. Tom, R. Rosario, *Empirical Mode Decomposition Based Features for Diagnosis and Prognostics of Systems*, Army Research Laboratory, 2008

[29] K. K.L. Ho, G.B. Moody, Peng C.-K., Mietus J.E., Larson M.G., Levy D., Goldberger A.L., *Predicting survival in heart failure case and control subjects by use of fully automated methods for deriving nonlinear and conventional indices of heart rate dynamics*, Circulation 1997

[30] E. Whitley, J. Ball, *Statisticsreview 3: Hypothesis testing and P values*, Critical Care, Vol. 6 No 3, 2002

[31] Grivell R.M., Alfirevic Z., Gyte GML., *Devane D., Antenatal cardiotocography for fetal assessment (Review)*, The Cochrane Library, 2010

[32] B. Knoll, *A Machine Learning Perspective on Predictive Coding with PAQ8 and New Applications*, The University of British Columbia, 2009